A study of pathophysiological roles of immune system-related receptors that regulate intestinal mucosal barrier function in inflammatory bowel disease model

This thesis was submitted to the

Graduate School of Medicine and Pharmaceutical Sciences

University of Toyama

to the fulfillment of a degree of

Doctor of Philosophy in Pharmaceutical Sciences.

Ai Hertati

Division of Gastrointestinal Pathophysiology

Institute of Natural Medicine

Graduate School of Medicine and Pharmaceutical Sciences

University of Toyama

Japan

December 2020

炎症性腸疾患モデルにおける腸管粘膜バリア機能を制御する免疫系受容体の病態生理学的役割に関する研究

Ai Hertati

富山大学

和漢医薬学総合研究所

病態制御部門

消化管生理学分野

2020 年 12 月

Contents

Abstract

Inflammatory bowel disease (IBD) is known as a complex and multifactorial disease which caused by combination between dysfunction of intestinal mucosal barrier, dysregulation of immune system, and inappropriate response to environmental factor such as gut microbiota in genetically susceptible host.

Intestinal mucosa acts as a selective barrier that allows nutrients absorption and at the same time restraint antigen uptake from the luminal side to the maintenance of intestinal mucosal homeostasis. The intestinal mucosal barrier function is orchestrated by intestinal environmental factors and cellular networks including epithelial cells, mesenchymal cells, immune cells and neuronal cells. Cytokines and short chain fatty acids (SCFAs) are key players in the regulation of cellular networks in the intestine via immune system-related receptors expressing on the various types of cells that constitute intestinal mucosa. Thus, the breakdown of intestinal mucosal barrier has been shown to play a critical role in the pathogenesis of intestinal immune-related disorders including IBD. However, the precise roles and networks between cytokines, SCFAs and immune system-related receptors in the intestinal mucosal barrier in vivo remain unclear.

Interleukin (IL)-4 and IL-13 are multifunctional and central cytokines in type 2 immune responses. These cytokines signal through the IL-4 receptor (IL-4R) system, which consists mainly of the IL-4Rα subunit. IL-4Rα subunit has been reported to express in various types of cells such as epithelial cells, macrophages and neuronal cells. Several studies showed evidences that IL-4 and IL-13 were involved in the regulation of intestinal mucosal barrier function through IL-4Rα signaling. However, there is no direct evidence has revealed the role of IL-4Rα in intestinal mucosal barrier function in vivo.

Recently, SCFAs produced by gut microbiota have been reported to maintain intestinal homeostasis through the activation of SCFA-sensing G protein-coupled receptors such as GPR41 and GPR43. It has been reported that GPR41 and GPR43 colocalize in enteroendocrine cells as sensors for SCFAs. GPR41 was also expressed in cell bodies of enteric neurons. However, there is no information available concerning which type of enteric neuron GPR41 is located. Furthermore, several studies showed the physiological and

pathophysiological roles of GPR41 and GPR43 in the gut using knockout mice. However, the precise roles of GPR41 and GPR43 are still controversial, and many questions regarding the functions of these receptors remain unanswered.

Therefore, the present studies investigated the role of IL-4Rα and morphological characterization of GPR41 immunoreactivity in the intestinal mucosal inflammation using murine IBD model.

1. IL-4Rα subunit deficiency protects mice from DSS-induced colitis through the enhancement of intestinal mucosal barrier function

In IBD patients, lamina propria mononuclear cells (LPMCs) in inflamed colonic mucosa produce large amounts of IL-13 compared with LPMCs in noninflammatory control patients. The expression of IL-4Rα was detected in the colonic enterocytes of IBD patients. Furthermore, IL-4- and IL-13-mediated intestinal epithelial barrier dysfunction was improved in mice lacking signal transducer and activator of transcription 6, a downstream effector of IL-4Rα activation. Although these findings suggest the involvement of IL-4Rα signaling in the disruption of intestinal mucosal barrier function in IBD patients, the precise role of the IL-4Rα in intestinal inflammation remains unclear.

This study was conducted to investigate the role of IL-4Rα during murine intestinal inflammation. To achieve this objective, IL-4Rα-deficient (IL-4Rα-/-) mice and their littermate wild-type (WT) mice were used. Experimental colitis was induced by administration of 3% dextran sulfate sodium (DSS) in the drinking water for 7 days. Treatment with DSS caused body weight loss, an increase in the disease activity index, colon shortened, and histological abnormalities in WT colitis mice, all of which were significantly attenuated in IL-4Rα-/- colitis mice. Neutrophil infiltration in the colonic mucosa was reduced in IL-4Rα-/- colitis mice compared with WT colitis mice. The increase in *Cxcl2* and *Il-1β* mRNA expression induced by DSS treatment was significantly suppressed in IL-4Rα-/- colitis mice. These results clearly demonstrate that the development of DSS-induced colitis

is suppressed in IL-4Rα-/- mice compared with WT mice. To investigate changes in colonic gene expression levels between WT colitis and IL-4Rα-/- colitis mice, I performed transcriptome analysis on colonic tissues. The differential expression analysis showed that the expression level of 47 genes was differentially expressed between IL-4Rα-/- colitis and WT colitis mice. Among the differentially expressed genes, I focused on *Nox1* expression because NOX1 has been reported to contribute to the maintenance of intestinal homeostasis. Consistent with the transcriptome analysis result, the qPCR analysis results showed that the *Nox1* mRNA expression was significantly higher in the colons of IL-4Rα-/- colitis mice. Furthermore, the depletion of IL-4Rα resulted in increase of *Nox1* mRNA expression level in the colons of normal mice. To determine the contribution of IL-4Rα to NOX1 activity, I measured reactive oxygen species (ROS) production in the murine colonic tissues. The ROS production was markedly higher in the colons of IL-4Rα-/- mice compared with WT mice in the both steady and colitis state. Since NOX1-dependent ROS production in intestinal epithelial cells is considered an important property for maintaining intestinal barrier, I hypothesized that IL-4Rα mediates intestinal mucosal barrier function through the regulation of NOX1-dependent ROS production. To address this hypothesis, I evaluated intestinal barrier function by intestinal permeability assay. IL-4Rα-/- mice showed a reduction in intestinal permeability, suggesting that the intestinal mucosal barrier function of IL-4Rα-/- mice may be strengthened by upregulation of NOX1-derived ROS production.

These findings indicate that IL-4Rα deficiency enhances intestinal mucosal barrier function through the upregulation of NOX1-dependent ROS production, thereby suppressing the development of DSS-induced colitis.

2. Morphological investigation of GPR41-positive enteric sensory neurons in the colon of mice with DSS-induced colitis

Previous reports have exhibited that dysbiosis of the gut microbiota is associated with aberrant immune response, intestinal barrier disruption and IBD. SCFAs are known as a group of molecule that involved in the crosstalk between microbiota, epithelial cells, and immune system. Growing evidence showed that sensory neurons in the enteric nervous system are involved in the pathological alteration of immune responses in IBD. Nevertheless, correlation between dysbiosis and enteric sensory neurons in the pathogenesis of IBD remain elusive.

Therefore I investigate the distribution of GPR41 and calcitonin gene-related peptide (CGRP) in the colonic mucosa of mice during intestinal barrier function disturbances. Disruption of intestinal barrier was induced by acute colitis model using DSS and antibiotic treatment. In the present study GPR41 was detected in nerve fiber and cell somas of enteric neurons. CGRP-immunoreactivities (IRs) were observed in the colonic lamina propria and enteric neurons. GPR41- and CGRP-IRs were markedly upregulated in the colitis mice compared to the normal mice. GPR41-IRs is partly colocalized with CGRP-IRs in the colonic lamina propria and muscularis layer of normal mice as well as colitis mice. This result indicated that GPR41 is located in the nerve fibers and cell somas of cholinergic intrinsic sensory neurons in the mouse colon. Antibiotic treatment for 10 days induced dysbiosis in mice which showed by cecum enlargement. However, antibiotic treatment failed to affect the morphology of small intestine and colon, and to cause antibiotic-induced diarrhea. Immunohistochemical analyses exhibit significant reduction of GPR41- and CGRP-IRs in the lamina propria of antibiotic-treated mice. In accordance with previous study, reduction of GPR41 immunoreactivities is probably due to alteration of gut microbiota composition after antibiotic treatment. These alterations were also accompanied by significantly decreased SCFAs, which probably lead to downregulation of GPR41 immunoreactivities. GPR41 and CGRP were found colocalized in the colonic lamina propria of vehicle and

antibiotic-treated mice. In addition I found that a number of GPR41-positive nerve fibers were in close proximity with F4/80-positive intestinal macrophages.

In conclusion, these findings suggest that GPR41-positive nerve fibers might be acted as a mediator in the crosstalk between host immune system and the gut microbiota and neuro-immune interaction were showed by the GPR41-positive nerve fibers juxtaposed with F4/80-positive intestinal macrophages.

Conclusion

Given the findings of my present studies, I conclude that IL-4Rα deficiency enhances NOX1-dependent ROS production and intestinal mucosal barrier function, resulting in the suppression of colitis development. In addition, GPR41 is suggested to act as a crosstalk mediator between gut microbiota and neuro-immune interaction in the intestinal mucosal barrier. Furthermore, the role of IL-4Rα and morphological alteration of GPR41 in the intestinal inflammation revealed here may improve the understanding of the pathogenesis of IBD.

Abbreviations

IBD: inflammatory bowel disease

CD: Crohn's disease

UC: ulcerative colitis

DSS: dextran sulfate sodium

IL-4Rα: interleukin 4 receptor alpha

GPCRs: G protein-coupled receptors

GPR41: G protein-coupled receptor 41

CGRP: calcitonin gene-related peptide

SCFA: short-chain fatty acid

IL: interleukin

mRNA: messenger RNA

DAI: disease activity index

H&E: hematoxylin and eosin

MPO: myeloperoxidase

IRs: immunoreactivities

ABX: antibiotic

Introduction

Inflammatory bowel disease

Inflammatory bowel disease (IBD) is a chronic idiopathic disorder causing inflammation in the gastrointestinal tract (Baumgart and Carding, 2007). IBD is characterized by the repeated alternating cycles of clinical relapse and remission (Lee et al., 2018). IBD patients exhibit symptoms such as bloody or non-bloody diarrhea, abdominal cramps, weight loss, and other features outside the gastrointestinal tract like skin rashes or arthritis. Diagnosis is based on clinical manifestation, endoscopic, and histological analysis. IBD consists of two main clinical forms, Crohn's disease (CD) and ulcerative colitis (UC). CD is characterized by discontinuous, transmural inflammation that can affect any part of the gastrointestinal tract, meanwhile, UC is presented as continuous mucosal inflammation that restricted to the colonic mucosal part (De Souza and Fiocchi, 2015; Levine et al., 2011).

The number of IBD patients has become increasing fast in the last two decades and become the world health burden. In North America and Europe, over 1.5 million and 2 million people suffer from the disease, respectively. In the countries which are influenced by a western European cultural heritage, including the USA, Canada, Australia, New Zealand, and all countries in western Europe) the number of patients also increasing (Ng et al., 2017; Benchimol et al., 2011; Benchimol et al., 2014). The increasing incidence of IBD in newly industrialized countries of Asia, South America, and Africa were the people become more westernized in lifestyle (Ng et al., 2017). This increasing of patients number brings challenges to the health care system around the world due to the capability of IBD to reduced quality of life, work capacity, and also increase disability (Alatab et al., 2020). In Japan, the accumulative number of IBD patients also increasing year by year (Okabayashi et al., 2020).

Although progress has been made in understanding IBD, their etiology is remains obscure. The fact that IBD needs long-term therapy and IBD is caused by multifactorial agent make this disease remain incurable. According to that condition, there is no exact treatment for IBD. The main goal of IBD treatment is to reduce inflammation that triggers the symptoms

to provide long-term remission as well as reduced risk of complication (Kumar et al., 2019; Neurath and Travis, 2012).

To achieve long-term remission, mucosal healing, and rebuilding of barrier function integrity in the intestinal mucosa is required (Neurath and Travis, 2012). This fact leads to an assumption that intestinal mucosal barrier function is crucial in IBD treatment.

Intestinal mucosal barrier function in IBD

Disruption of the intestinal mucosal barrier has been reported as one of IBD etiologic factor besides dysregulation of the immune system, inappropriate response to environmental factors such as gut microbiota in a genetically susceptible host (Sartor, 2006).

The gastrointestinal tract was protected by an intestinal mucosal barrier which comprised physical barrier, and chemical barrier (Figure 1). A functional intestinal mucosal barrier acts as a selective barrier by allows absorption of nutrients and fluids but simultaneously prevents harmful substances like toxins and bacteria from passing through the intestinal epithelium to the underlying tissue (Schoultz and Keita, 2020; Furness et al., 1999). The physical barrier comprises the mucus layer, glycocalyx, and the cell junction that thoroughly linking intestinal epithelial cells. The mucus layer forms a protected habitat for the commensal microbiota in close proximity to the epithelial cells (Cornick et al., 2015; Smith et al., 2009). The mucus layer consists of IgA, one of the most abundant antibodies in the mucosal secretion that neutralize pathogenic bacteria and favor maintenance of commensal microbiota (Gutzeit et al., 2014). The physical barrier protects the mucosa from intestinal microorganism aggression. The next part of the intestinal mucosal barrier is the epithelium, a single layer that separates the body from the external lumen side. The epithelium is composed of several different cell types, such as enterocytes, Paneth cells, and goblet cells (Schoultz and Keita, 2019). Lamina propria is underlain below the epithelial cells consist of innate and adaptive immune cells such as macrophages, B cells, and T-regulatory cells (Santaolalla et al., 2011; Okumura and Takeda, 2017). Chemical barriers, which include antimicrobial peptide (AMP), regenerating islet-derived 3 family of protein, lysozyme, and secretory phospholipase A2 (Okumura and Takeda, 2017; Quiros and Nusrat, 2019).

Cytokines and short-chain fatty acids (SCFAs) play pivotal roles in the intestinal mucosal cellular networks through the activation of immune system-related receptors expressing on the various types of cells (Friedrich M et al., 2019; D'Souza et al., 2017). To understand the intestinal mucosal barrier function, it is important to reveal the precise roles of these receptors.

The current study investigates two kinds of receptors related to intestinal mucosal barrier function which are cytokine receptor interleukin-4 receptor alpha (IL-4Rα) and SCFAs receptor, G protein-coupled receptor 41 (GPR41).

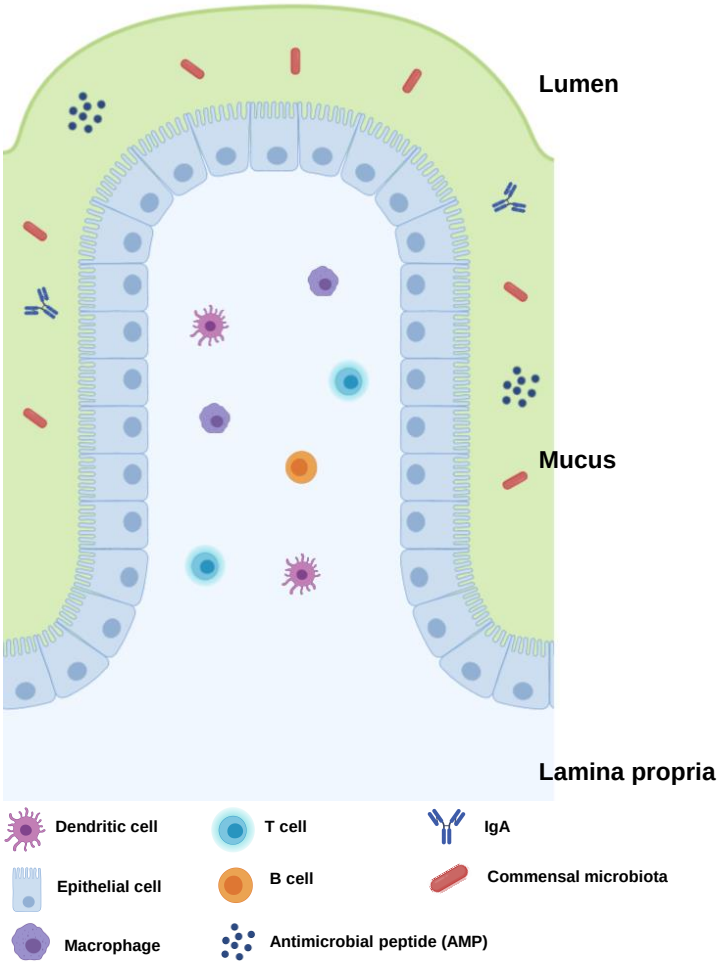

Figure 1. Schematic presentation of intestinal mucosal barrier that protects our gastrointestinal tract, comprises of the physical and chemical barrier.

IL-4Rα

IL-4Rα is the main receptor unit for major Th2 cytokines IL-4 and IL-13 (Egholm et al., 2019; LaPorte et al., 2008). The IL-4Rα consists of a 140 kDa IL-4Rα chain which is a main comnponent of both type I and type II receptors. Type I receptor is comprised of IL-4Rα chain and γchain subunit, meanwhile type 2 receptor contain IL-13Rα1 besides IL-4Rα (Nelms et al., 1999) (Figure 2). IL-4Rα subunit has been reported to express in various types of cells such as epithelial cells (Takeda et al., 2010), macrophages (Jenkins et al., 2013), and neuronal cells (Lee et al., 2018). Several studies showed evidence that IL-4 and IL-13 were involved in the regulation of intestinal mucosal barrier function through IL-4Rα signaling (Groschwitz and Hogan, 2009). In IBD patients, inflamed colonic mucosa produces large amounts of IL-13 compared with noninflammatory control patients (Heller et al., 2005). Furthermore, expression of IL-4Rα was detected in the colonic enterocytes of IBD patients (Heller et al., 2005).

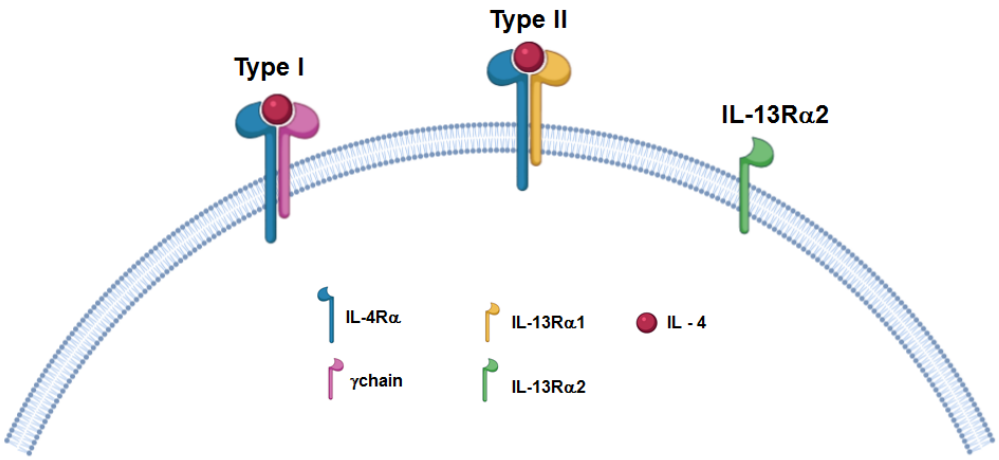

Figure 2. IL-4 receptor complex. IL-4 interact with type I and type II receptor complex.

GPR41

The second receptor is SCFA-sensing G protein-coupled receptor GPR41. GPR41 is one of the SCFA receptors besides GPR43 and GPR109a. GPR41 was deorphanized in 2003 and activated by SCFAs such as acetate (C2), propionate (C3), butyrate (C4) and valerate (C5)

which generated by gut microbiota fermentation of dietary fibers in the colon (Le Poul et al., 2003; Brown et al., 2003). GPR41 has been reported to express in various tissues, including adipose tissues, intestines, peripheral nervous system, and immune cells. Their existences showed their crucial role in the regulation of energy homeostasis via SCFA (Brown et al., 2003; Kimura et al., 2011; Le Poul et al., 2003; Samuel et al., 2008). SCFAs are one of the molecules involved in the crosstalk between gut microbiota, epithelial cells, and the immune system (Sheppach, 1994; D'Souza et al., 2017). SCFA will bind to these receptors and exert their function in the physiological and pathophysiological conditions. For examples, regulating the intestinal motility, hormone secretion, maintenance of intestinal mucosal barrier, and immune cell function (Priyadarsini et al., 2018; D'Souza et al., 2017; Le Poul et al., 2003; Brown et al., 2003; Nilsson et al., 2003; Thangaraju et al., 2009). Several previous studies have shown the protective roles of SCFAs in IBD models via the activation of GPR43 (Arpaia et al., 2013; Maslowski et al., 2009; Masui et al., 2013).

DSS colitis model

Dextran sulfate sodium (DSS) is the most widely used to make chemically induced colitis model. DSS is a chemical colitogen, possesses anticoagulant properties, to induced disease. DSS is water-soluble, negatively charged, with a variety of molecular weights ranging from 5-1400 kDa. The most severe murine colitis, which most resemblance human UC was generated by administered 40-50 kDa DSS in drinking water (Okayasu et al., 1990; Chassaing et al., 2015). The mechanism of how DSS induced intestinal inflammation is unclear but is presumed caused by the destruction of epithelial monolayer lining the large intestine allowed translocation of pathogenic bacteria and their metabolite into underlying tissue. The DSS-induced acute colitis is very popular because the model is simple, reproducible, rapid, and easy to control. Different types of intestinal inflammation, such as acute, chronic, and relapsing models could be addressed by modifying DSS concentration and administration frequency (Chassaing et al., 2015).

Evaluation of acute DSS-induced colitis model is carried out by daily monitoring of body weight, stool consistency, and the presence of blood in the stool which could be summarized

as disease activity index (DAI) score. In the beginning, mice body weight might slightly increase depend on DSS dosage and mouse strain. Mice with lower resistance to DSS exhibit severe rectal bleeding and weight loss within 3-4 days of DSS administration. In accordance with Guide for the Care and use of Laboratory Animals of the National Institute of Health, we have to set the humane endpoint based on the percentage of body weight loss (Chassaing et al., 2015). Histological changes induced by DSS include mucin and goblet cell depletion, epithelial erosion, and ulceration are quantitatively determined by histological score. Furthermore, DSS also induced an influx of neutrophils into the lamina propria and submucosa and increase proinflammatory cytokine expression such as IL-1β, TNFα, IL-6, IFNγ and Cxcl2 (Yan et al., 2009; Perše and Cerar, 2012; Chassaing et al., 2015; Melgar et al., 2005; Hayashi et al., 2017; Farooq et al., 2009).

Antibiotic-induced dysbiosis model

Antibiotic-induced dysbiosis models has been used to investigate the role of gut microbiota in some pathological conditions (Zarrinpar et al., 2018; Sampson et al., 2016; Shen et al., 2015; Rakoff-Nahoum et al., 2004). The effect of low-dose antibiotic treatment induced dysbiosis through decreasing gut microbiota diversity (Zarrinpar et al., 2018; Mahana et al., 2016; Cho et al., 2012; Cox et al., 2014). Epidemiological studies unveil that antibiotics treatment increases the risk of IBD. It remains unknown how antibiotic-induced dysbiosis confers the risk of increasing inflammatory response (Holota et al., 2019). However the impact of microbiota depletion on metabolic homeostasis is still not well characterized and showed the paradoxical impact. For instance, gut microbiota is responsible to generate extra calories through fermentation of dietary fibers into SCFAs (Zarrinpar et al., 2019; Canfora et al., 2015). Consequently, gut microbiota depletion could result in a decrease number of calories and decreased luminal SCFAs (Zarrinpar et al., 2019; Wichmann et al., 2013; Bäckhed et al., 2007).

Objective

Interaction between intestinal environmental factors and cellular networks across epithelial cells, immune cells, mesenchymal cells, and neuronal cells construct a complex structure that organized intestinal mucosal barrier function. There are two main players in the regulation of intestinal cellular networks, which are cytokines and SCFAs. They exert the regulation function through intestinal immune system-related receptors that are expressed on various cell types that build the intestinal mucosal barrier. Disruption of the intestinal mucosal barrier has been shown involved in intestinal immune-related diseases including IBD. However, the precise roles and the networks between cytokines, SCFAs, and immune system-related receptors in the intestinal mucosal barrier function in vivo remain obscure.

To gain a better understanding of the interaction between cytokine, SCFAs, and immune system-related receptors in the pathogenesis of IBD, we investigated the role of IL-4Rα and SCFA-sensing G protein-coupled receptor GPR41 in the regulation of intestinal mucosal barrier function that involves in the pathogenesis of intestinal inflammation using murine IBD model (Figure 3).

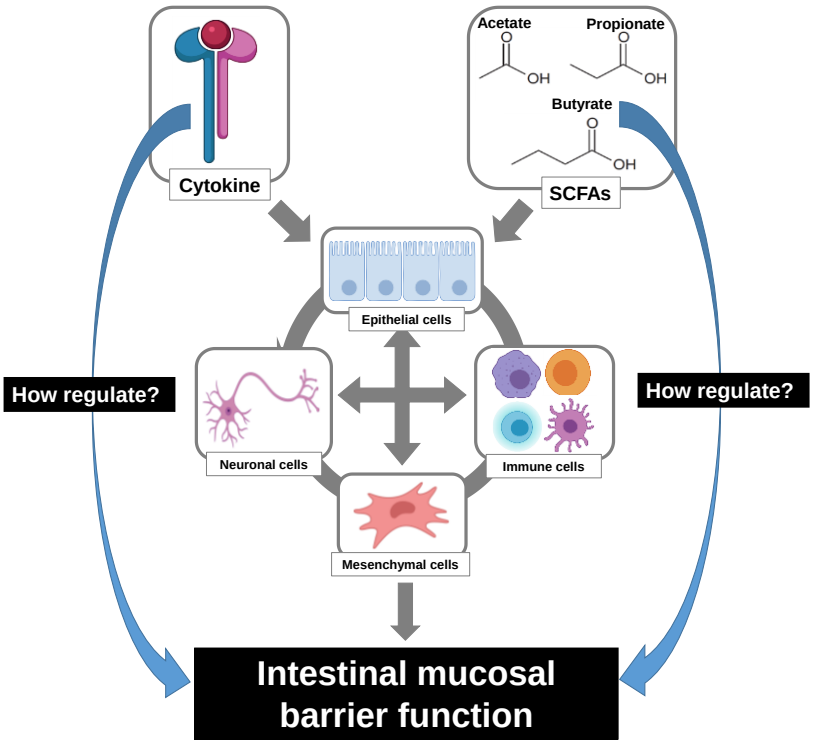

Figure 3. The aim of my study to investigate the role of a cytokine receptor, IL-4Rα, and SCFAs receptor, GPR41, in the regulation of intestinal mucosal barrier function in the inflammatory bowel disease model.

Chapter 1

IL-4 receptor α subunit deficiency protects mice from DSS-induced colitis through enhancement of intestinal mucosal barrier function

1. Introduction

IL-4 and IL-13 are multifunctional and central cytokines in type 2 immune responses (Egholm et al., 2019). These cytokines exert their function through the IL-4 receptor system, which comprises of type 1 (heterodimer between IL-4Rα and γchain) and type 2 (heterodimer between IL-4Rα and IL-13Rα1) (Nelms et al., 1999). IL-4Rα has been reported to express in various type of cells including epithelial cells, (Takeda et al., 2010), tissue-resident macrophages (Jenkins et al., 2013), and neuronal cells (Lee et al., 2018). Previous reports showed evidence that IL-4 and IL-13 contribute to the regulation of the intestinal mucosal barrier function (Groschwitz and Hogan, 2009). Stimulation of human colonic epithelial monolayer cells by IL-4 and IL-13 reported could increase intestinal permeability (Zünd et al., 1996; Berin et al., 1999). Another report demonstrated improvement of intestinal epithelial barrier function through IL-4 and IL-13 in STAT6 deficient mice (Madden et al., 2002). Furthermore, the inflamed colonic mucosa of UC patient's produces large amounts of IL-13 in the lamina propria mononuclear cells (LPMCs) compared with LPMCs in non-inflammatory control patients (Heller et al., 2005). These finding suggested the roles of IL-4Rα in the intestinal inflammation development through regulation of intestinal mucosal barrier function.

Intestinal mucosal barrier was defined as complex structure that separates the internal milieu from the luminal environment (Cummings et al., 2004; Bischoff et al., 2014). The intestinal mucosal barrier consists of physical and chemical barriers that regulated by intestinal environmental factors and cellular networks including epithelial cells, mesenchymal cells, immune cells, and neuronal cells (Okumura and Takeda, 2017; Friedrich et al., 2019). The intestinal mucosal surface is coated by a thick mucus gel comprise of the

outer layer that secreted mucins, the inner layer of the glycocalyx, and cell junctions (Hooper and Macpherson, 2010; Okumura and Takeda, 2017; Friedrich et al., 2019). Besides provided physical barrier, intestinal mucosa also plays the role as a chemical barrier through the generation of antimicrobial peptides (AMPs), which includes lysozymes, defensins, cathelicidins, lipocalins, and also C type lectin such as RegIIIg (Koslowski et al., 2010; Okumura and Takeda, 2017; Friedrich et al., 2019). Intestinal mucosa act as a selective barrier that allows nutrients absorption and limits the uptake of antigens from the lumen at the same time (Quiros and Nusrat, 2019). The intestinal mucosa prevents enormous contact of antigens with the immune cells and thereby protect the gut from an aberration of the immune response (Martini et al., 2017). Cytokines and their receptors act together at the cellular interaction in the intestine under both physiological and pathophysiological conditions (Friedrich et al., 2019).

However, the role of IL-4Rα in murine intestinal inflammation related to intestinal barrier function remains unclear. Thus, in recent research, I determine the role of IL-4Rα in the intestinal inflammation using an experimental acute colitis model induced by DSS using IL-4Rα-/- mice.

2. Materials and methods

2.1. Animals

IL-4Rα-/- mice (BALB/cJ-*il4ratm1Sz*) on a BALB/c background (Noben-Trauth et al., 1997) were purchased from Taconic Biosciences (Rensselaer, NY, USA). To generate WT and IL-4Rα-/- littermate for the experiments, IL-4Rα hetero-deficient mice were crossed and confirmed by genotyping (Figure. 4A). Mice were housed in a room with a light/dark cycle (12 h: 12 h) in the experimental animal facility at the University of Toyama and were provided free access to food and water. All experiments were performed in accordance with the Guide for the Care and Use of Laboratory Animals of the National Institute of Health and the University of Toyama. The Animal Experiment Committee at the University of Toyama approved all of the animal care procedures and study protocols (authorization No.

A2015INM-2 and A2018INM-3). In this study, I used 10-12 weeks old male mice, 16 mice in each normal group, and 24 mice in each colitis group.

2.2. Genotyping

To determine genotype of littermates, PCR was performed using primer pairs specific for exon 7 and the *neo* gene in a single reaction according to the previous report (Noben-Trauth et al., 1997). DNA was extracted from the tails of mice using DirectPCR Lysis Reagent (Viagen Biotech, Los Angeles, CA, USA) according to the manufacturer's instructions. PCR amplification was performed using MightyAmp DNA polymerase (Takara Bio). The PCR conditions were as follows: initial denaturation at 98°C for 2 minutes, followed by 25 cycles of amplification (98°C for 10 seconds, 60°C for 15 seconds and 68°C for 1 minute). A portion of the PCR mixture was electrophoresed on 2% agarose gel containing 0.1% ethidium bromide in Tris-borate-EDTA buffer and photographed.

2.3. DSS-induced acute colitis model

Mice were administered with 3% DSS (36-50 kDa; MP Biomedical, Santa Ana, CA, USA) in drinking water for 7 days based on a previous report (Hayashi et al., 2017). Assessment of colitis severity was made by daily observation of body weight, stool consistency, and presence of blood in the stool. The disease activity index was the average of 2 parameters: diarrhea (0, normal; 1, soft stool; 2, loose stool; 3, mild diarrhea; 4, severe diarrhea) and blood in the stool (0, normal; 1 faint bleeding; 2, slight bleeding; 3 gross bleeding; 4, severe bleeding). DSS-induced acute colitis model was terminated when body weight loss reached 20% of initial body weight as the humane endpoint.

2.4. Histology analysis

Histology analysis was performed in accordance with previous report (Hayashi et al., 2014). In brief, the distal colon was fixed in 4% paraformaldehyde for 24 hours at 4°C, treated with 30% sucrose solution, then embedded in Tissue Freezing Medium (TBS, Durham, NC, USA). The frozen sections were sliced into 10 μm thickness at -20°C using a cryostat microtome

(Leica Microsystem, Nussloch, Germany). The sections were routinely stained with hematoxylin and eosin (H&E). H&E-stained sections were score for inflammation and crypt damages based on our previous report (Hayashi et al., 2014).

2.5. Immunohistochemistry analysis

Immunohistochemistry was performed as described in the previous report (Lee et al., 2013) with slight modification. In brief, the mice were sacrificed on day 7 after DSS administration and distal colons were isolated, fixed in 4% paraformaldehyde for 2 hours at 4°C and treated with 30% sucrose solution. The tissue sample was embedded in an OCT compound (Sakura Finetek, Tokyo, Japan). Frozen sections (30 μm) were immersed for 1 hour in 0.3% Triton X-100 solution and exposed to normal donkey serum (1:10; Jackson ImmunoResearch Laboratories, West Grove, PA, USA) for 1 hour at room temperature. The sections were incubated with rabbit anti-human myeloperoxidase (MPO) antibody (1:200; Abcam, Cambridge, UK) or rabbit anti-IgG antibody (Wako, Osaka, Japan) for isotype control of MPO antibody (Figure. S2) and then incubated with Alexa Fluor 488-conjugated donkey anti-rabbit IgG (1:400); Jackson ImmunoResearch Laboratories). The sections were mounted using VECTASHIELD mounting medium containing DPI (Vector Laboratories, Peterborough, UK). The stained sections were observed and visualized using a confocal laser-scanning microscope (LSM780; Carl Zeiss, Oberkochen, Germany). The number of MPO-positive cells in the colonic mucosa was determined using ImageJ software (NIH, Bethesda, MD, USA).

2.6. RNA isolation and quantitative real-time PCR (qPCR)

Total RNA was isolated from mouse colon using Sepasol RNA I Super (Nacalai Tesque, Kyoto, Japan) according to the manufacturer's instruction. Transcript levels of *Il-1β, Cxcl2, Nox1, Il-4, Il-13,* and *Il-4rα* were determined as described in the previous report (Hayashi et al., 2017). I generated cDNA using PrimeScript RT Reagent Kit (Takara Bio, Ohtsu, Japan) and amplify it by qPCR using TB Green Premix EX Taq (Takara Bio). qPCR was performed using Takara TP800 (Takara Bio). The PCR reaction conditions consisted of 10 seconds at

95°C and 20 seconds at 60-63°C. Relative mRNA expression was normalized to *Gapdh* as an internal control in each sample. The results are expressed as a ratio relative to the average of the control group. The primers are shown in Table 1.

Table 1. **Primer sequences for qPCR**

	Primer sequence, 5'-3'	
Gene	**Forward**	**Reverse**
Gapdh	TGACCACAGTCCATGCCATC	GACGGACACATTGGGGGTAG
Cxcl2	ACCCCACTGCGCCCAGACAGAA	AGCAGCCCAGGCTCCTCCTTTCC
Il-1β	CTGTGTCTTTCCCGTGGACC	CAGCTCATATGGGTCCGACA
Il-4	GGTCTCAACCCCCAGCTAGT	GCCGATGATCTCTCTCAAGTGAT
Il-13	GGATATTGCATGGCCTCTGTAAC	AACAGTTGCTTTGTGTAGCTGA
Il-4rα	ACGTGGTACAACCACTTCCA	TGGCTTCGGGTCTGCTTATC
Nox-1	AGTAGGTGTGCATATGGGTGT	ACCAGCCAGTTTCCCATTGT

2.7. Transcriptomic analysis

Transcriptomic analysis was conducted based on our previous report (Nagata et al., 2017). Briefly, total RNA was isolated from the distal colon after 7 days of 3% DSS treatment. mRNA was purified from the mixture of total RNA using RNeasy Mini Kit (Qiagen, Crawley, UK), and then mRNA of 3-6 mice from each group (WT normal, WT colitis, and IL-4Rα-/- colitis) was mixed. Microarray analysis was performed using GeneChip Mouse Gene 1.0 ST array (Affymetrix, Santa Clara, CA, USA). The GeneChip was scanned with GeneChip Scanner 3000 (Affymetrix), and the gene expression was analyzed using GeneChip Analysis

Suite Software (Affymetrix). Median centered and log2 transformed transcript levels are indicated by the color code: blue (low) and red (high). Moreover, the GeneChip microarray data set then analyzed using Transcriptome Analysis Console (TAC; Thermo Fisher Scientific, Waltham, MA, USA), GeneSpring (Silicon Genetics, Redwood City, CA, USA), and Ingenuity Pathway Analysis (IPA; Ingenuity Systems, Redwood City, CA, USA, http://www.ingenuity.com) to extract significant genes, and identify gene ontology and canonical pathways associated with the differentially expressed genes.

2.8. Isolation of colonic epithelial cells (CEC)

CEC was isolated by the chelation method using EDTA as described previously (Hayashi, 2014; Greten et al., 2004) with minor modification. Briefly, the colon was excised, open longitudinally then washed of fecal content in ice-cold RPMI-1640 (Wako, Osaka, Japan). The colons were then cut into small pieces and stirred at 37°C for 20 min in RPMI-1640 containing 2% FBS (GIBCO, Carlsbad, CA) and 0.5 mM EDTA. Then the colons tissue were separate from the solution by using 0.5 µ filter, centrifuge at 500 g for 7 min at 4°C.

2.9. Measurement of ROS production

Measurement of ROS production was performed following the previous report (Yokota et al., 2017). Whole colon tissues were isolated on day 7 after 3% DSS treatment from WT and IL-4Rα-/- mice then washed with ice-cold PBS. Tissue samples were then homogenized in ice-cold Krebs-HEPES buffer (pH 7.4) containing protease cocktail inhibitor (Complete Mini; Roche, Mannheim, Germany), and then centrifuged at 1100 x g at 4°C for 15 min. The production of ROS which is mainly superoxide was determined using chemiluminescence assay by L-012 (Wako, Osaka, Japan). Chemiluminescence was measured with a luminometer (Lumat LB 9507, Berthold Technologies, Germany). The level of ROS production was presented as arbitrary light units per minute per mg protein.

2.10. In vivo intestinal permeability assay

In vivo intestinal permeability assay was performed based on the previous report (Gupta et al., 2014) with a slight modification. Briefly, normal and colitis mice were fasted overnight. 200 mg/kg body weight of FITC-dextran (4 kDa, Chondrex, Redmond, WA, USA) was given by per oral administration. Control mice were administered with PBS (-). After 4 hours, mice were anesthetized and blood was collected by cardiac puncture. Blood samples were centrifuged (2500 x g, 10 min, 4°C) and plasma was collected. The fluorescence intensity of samples was measured in black 96-well plates by a microplate reader (Tecan GENios; TECAN, Männedof, Switzerland) at the wavelength 485 nm (excitation) and 535 nm (emission). FITC-dextran concentrations were measured from a standard curve.

2.11. Statistical analysis

The data are presented as the mean ± SEMs. Statistical analyses were conducted with Prism 8 (GraphPad Software, San Diego, CA) using one- or two-way ANOVA followed by Bonferroni's multiple comparison test or an unpaired t-test with Welch's correction. Probability (P) values <0.05 were considered statistically significant.

3. Results

3.1.Genotyping

I confirmed that the IL-4Rα expression was totally depleted in the colon of IL-4Rα-/- mice by performed PCR genotyping and qPCR. Gel electrophoresis of PCR genotyping showed PCR products with the size 125 bp band in WT mice, a 280 bp band in IL-4Rα-/- mice, and 125 bp and 280 bp bands in IL-4Rα-hetero-deficient (IL-4Rα+/-) mice (Figure 4A). qPCR analysis results showed the mRNA expression level of *Il-4rα* in the colons of IL-4Rα-/- normal mice were totally depleted (Figure 4B; n=4; $P<0.05$).

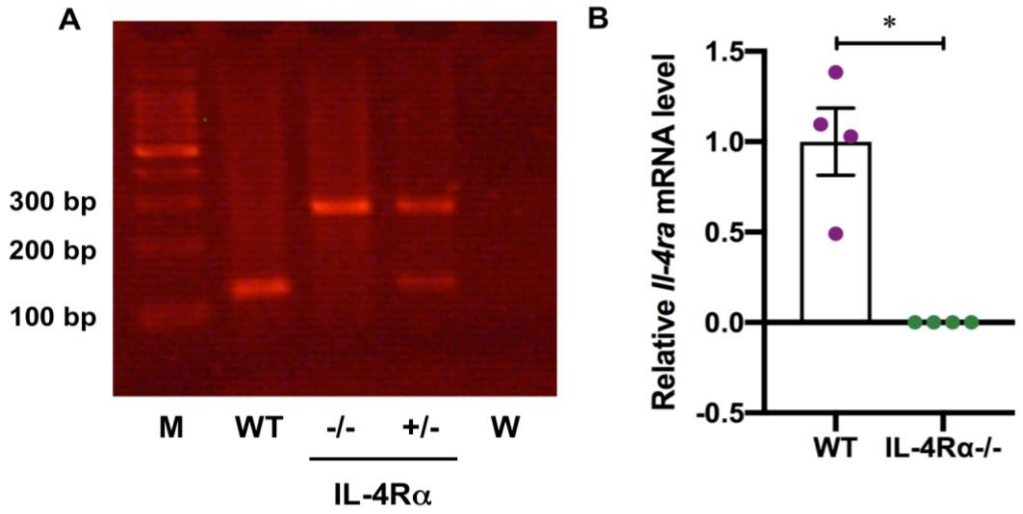

Figure 4. (A) Representative images of genotyping are shown. PCR products reveal a 125 bp band in WT mice, a 280 bp band in IL-4Rα-/- mice, and 125 bp and 280 bp bands in IL-4Rα-hetero-deficient (IL-4Rα+/-) mice. Water (W) was amplified as negative control template. M, molecular mass markers. (B) The mRNA expression level of *Il-4rα* in the colons of WT and IL-4Rα-/- normal mice. The data are presented as the mean ± SEM values for 4 mice. *p<0.05

3.2.IL-4Rα deficiency increased resistance to DSS-induced colitis

To investigate the role of IL-4Rα in murine intestinal inflammation, I use the DSS-induced acute colitis model in WT and IL-4Rα-/- mice. The loss of body weight was started on day 4 after DSS treatment, and it was markedly attenuated in IL-4Rα-/- colitis mice (Figure 5A; 78.5 ± 2.0% in WT colitis; 92.6 ± 1.4% in IL-4Rα-/- colitis mice on day 7; P<0.001).

The disease activity index was determined as the average of diarrhea score and rectal bleeding score and was also significantly alleviated in IL-4Rα-/- colitis mice (Figure 5B; 3.7 ± 0.2 in WT colitis; 1.1 ± 0.3 in IL-4Rα-/- colitis on day 7; P<0.001).

There is no difference in colon length of WT and IL-4Rα mice in normal mice. But, after 7 days DSS treatments, colon shortened was significantly attenuated in IL-4Rα-/- colitis

mice compared to WT colitis mice (Figure 6A, 6B; 7.5 ± 0.2 cm in WT colitis; 10.1 ± 0.5 cm in IL-4Rα-/- colitis; P<0.001).

Histology analysis by H&E staining revealed that DSS treatment for 7 days was caused the loss of epithelial integrity and crypt architecture in WT colitis mice which was accompanied by submucosal edema. All of this colon destruction was attenuated in IL-4Rα-/- colitis mice (Figure 6C, 6D; 5.5 ± 0.3 in WT colitis; 2.5 ± 0.2 in IL-4Rα-/- colitis; P<0.001).

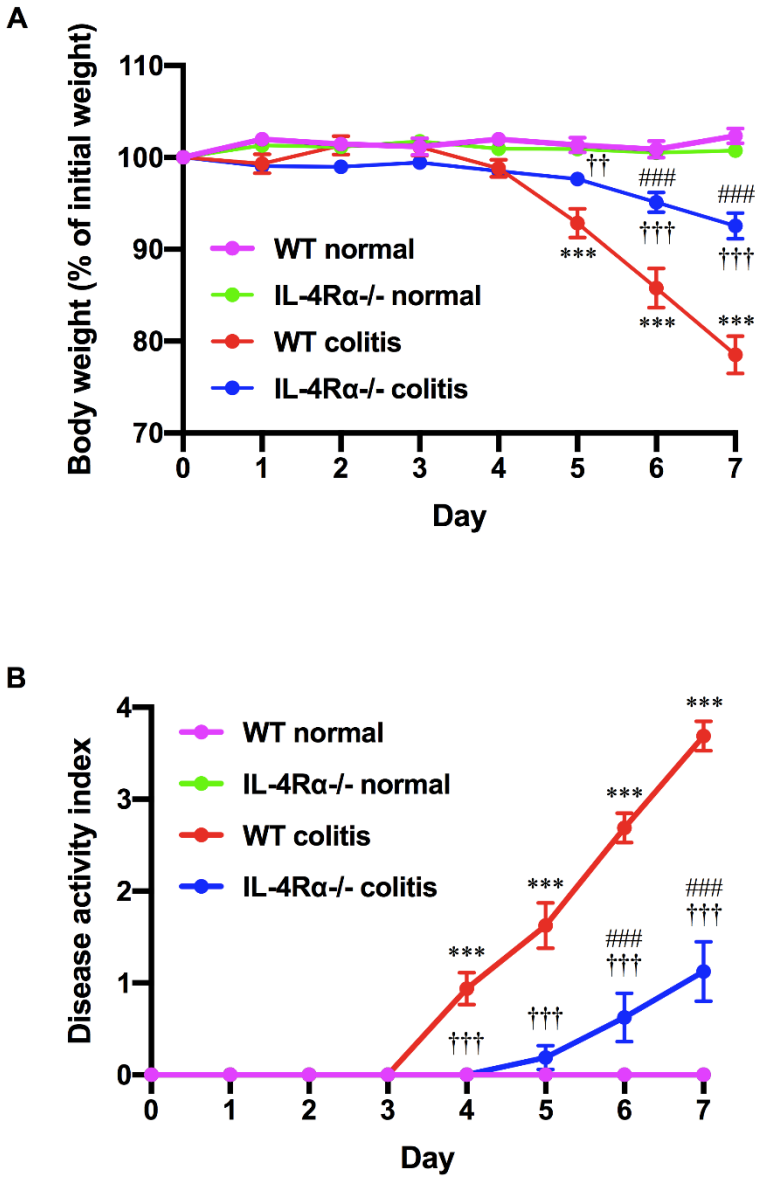

Figure 5. IL-4Rα deficiency increased resistance to DSS-induced colitis. Experimental acute colitis was induced in WT and IL-4Rα KO mice by giving 3% dextran sulfate sodium (36-50 kDa) in drinking water for 7 days. (A) Body weight loss, (B) disease activity index are shown. The data are presented as the mean ± SEM values for 8 mice and are representative of 1 of 3 independent experiments. ***p<0.001 compared with WT normal mice. ††p<0.01 and †††p<0.001 compared with WT colitis mice. ###p<0.001 compared with IL-4Rα-/- normal mice.

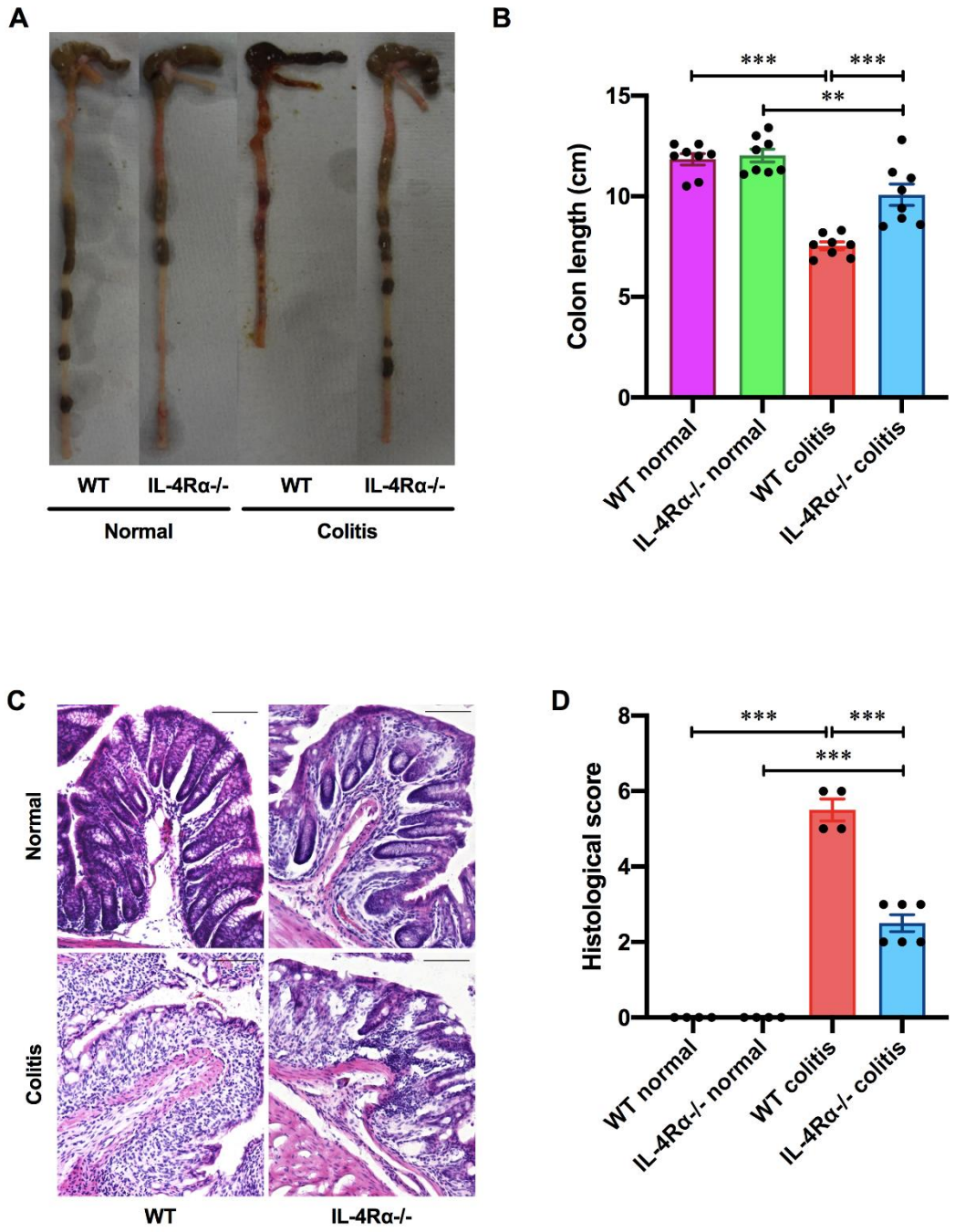

Figure 6. IL-4Rα deficiency increased resistance to DSS-induced colitis. Colitis was induced in WT and IL-4Rα-/- mice by daily treatment with a 3% DSS solution in the drinking water for 7 days. (A) Macroscopic photographs of colons and (B) colon length measurements are shown. The data are presented as the mean ± SEM values for 8 mice and are representative

of 1 of 3 independent experiments. **p<0.01; ***p<0.001. (C) Representative images of H&E staining are shown. The scale bar represents 100 μm. (D) Histological scoring of DSS-induced colitis is shown. The data are presented as the mean ± SEM values for 4-6 mice. ***p<0.001.

Furthermore, I investigated the MPO immunoreactivity to determine the distribution of neutrophils in the mice colonic mucosa after 7 days of DSS treatment. MPO immunoreactivities was markedly increased after DSS treatment in WT colitis mice (Figure 7A) and it was significantly decreased in IL-4Rα-/- colitis mice. I used IgG as an isotype control for MPO-immunoreactivity to confirm the unspecific binding (Figure 7B). Quantitative analysis was showed the infiltrated neutrophils were significantly reduced in IL-4Rα-/- colitis mice (Figure 7C; 169.9 ± 24.5 in WT colitis; 78.9 ± 11.7 in IL-4Rα-/- colitis; P<0.001).

The mRNA expression level of *Cxcl2* and *Il-1β* in the colons of WT colitis mice was markedly elevated on day 7 (Figure 8A; *Cxcl2*; 0.0 ± 0.0 in WT normal, 5.3 ± 1.7 in WT colitis; P<0.01, Figure 8B; *Il-1β*; 0.4 ± 0.1 in WT normal, 6.6 ± 2.1 in WT colitis; P<0.01). However, the increase in *Cxcl2* and *Il-1β* mRNA expression was significantly suppressed in the colons of IL-4Rα-/- colitis mice (Figure 8A; *Cxcl2*; 5.3 ± 1.7 in WT colitis, 0.5 ± 0.3 in IL-4Rα-/- colitis; P<0.05, Figure 8B; *Il-1β*; 6.6 ± 2.1 in WT colitis, 0.3 ± 0.1 in IL-4Rα-/- colitis; P<0.01). These results clarify that the development of DSS-induced colitis is suppressed in IL-4Rα-/- mice compared with WT mice.

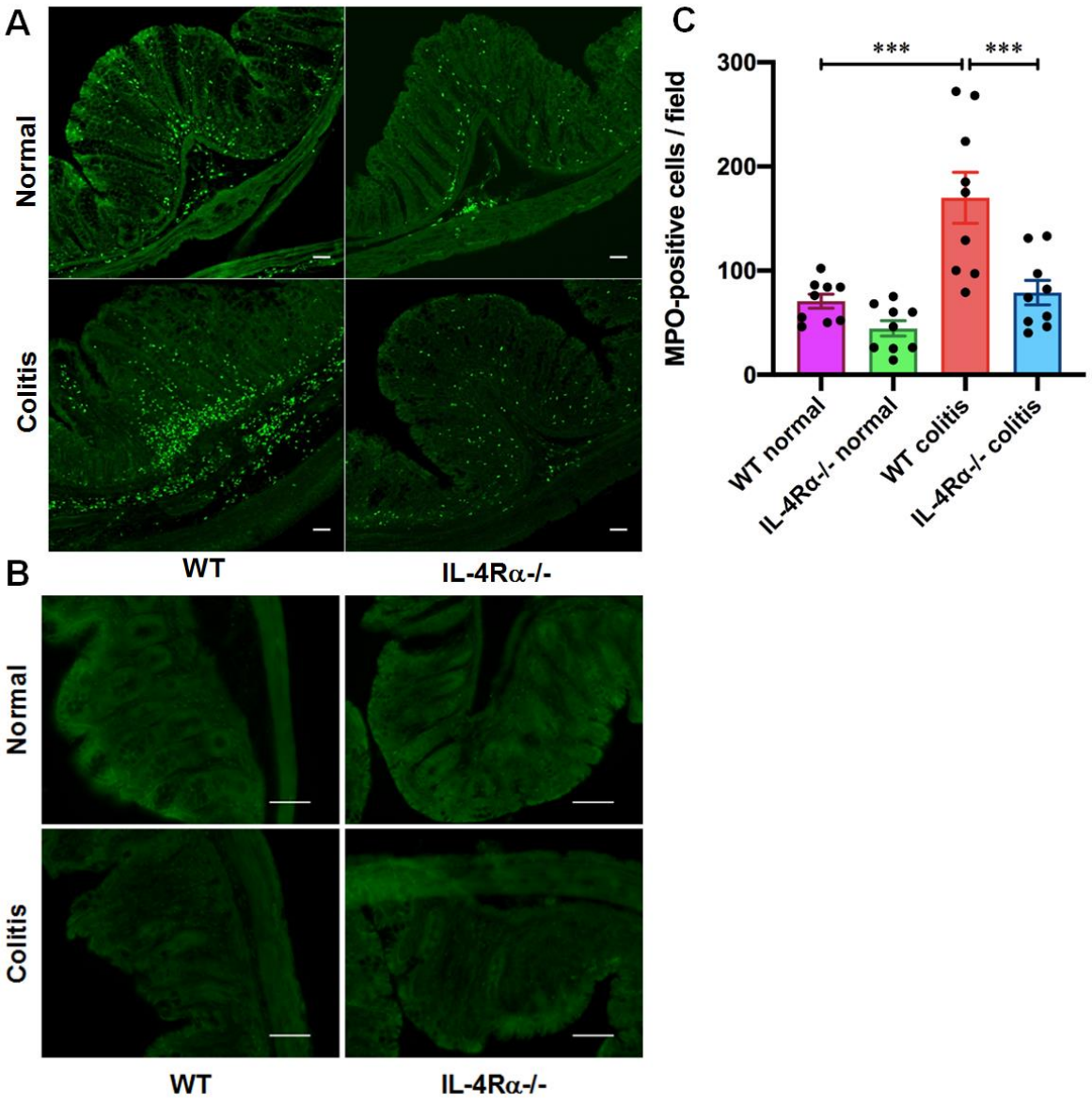

Figure 7. IL-4Rα-/- mice showed a low inflammatory response to DSS-induced colitis. Colitis was induced in WT and IL-4Rα-/- mice by daily treatment with 3% DSS solution in drinking water for 7 days. (A) Representative images of the confocal micrograph of the mice colonic mucosa showed staining of MPO-positive cells. The scale bar represents 50 μm. immunohistochemistry analysis results. (B) Representative images of isotype control IgG staining for MPO antibody are shown. The scale bar represents 100 μm. (C) The number of

MPO-positive cells in the colonic mucosa is shown. The data are presented as the mean ± SEM values for 9 mucosae from 3 mice. ***p<0.001

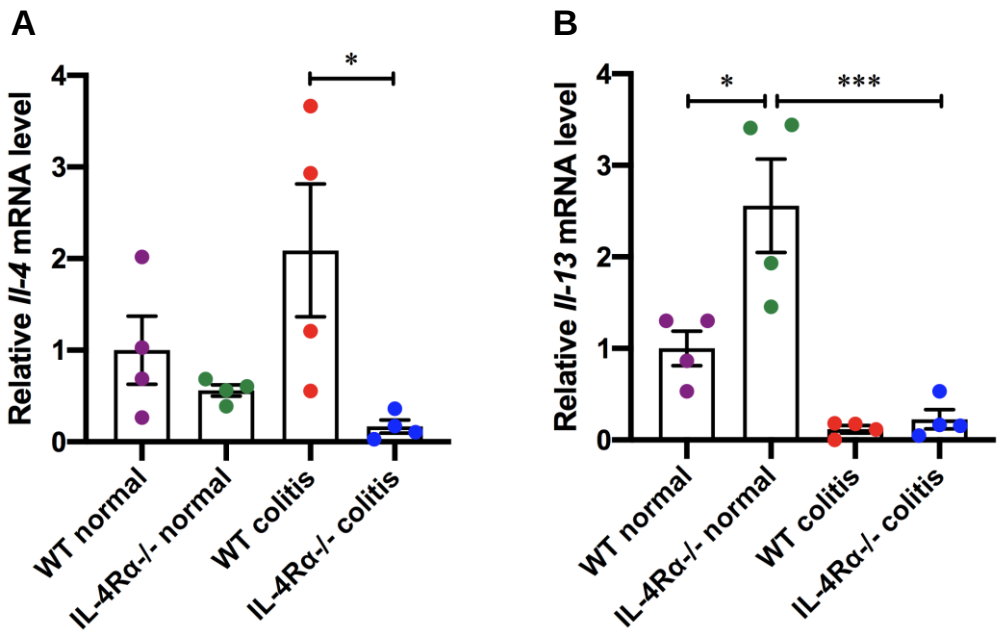

Figure 8. DSS-induced changes in the mRNA expression level of (A) *Cxcl2* and (B) *Il-1β* in the colons of WT and IL-4Rα-/- mice. The data are presented as the mean ± SEM values for 4 mice and are representative of 1 of 2 independent experiments. *p<0.05; **p<0.01.

3.3.IL-4Rα deficient mice elevated NOX1-dependent ROS production in the mouse colon

I investigate the changes in colonic gene expression levels in WT colitis and IL-4Rα-/- colitis mice by transcriptomic analysis of colon tissues collected on day 7 after 3% DSS treatment. The differential expression analysis using TAC showed that the expression level of 91 genes was altered by DSS treatment and 47 genes were differentially expressed between IL-4Rα-/- colitis and WT colitis mice (Figure 9A). Among 47 genes, 10 genes were upregulated and 37 genes were downregulated in IL-4Rα-/- colitis mice compared with WT colitis mice. Furthermore, the top 10 upregulated and downregulated genes in IL-4Rα-/- colitis mice compared to WT colitis mice were shown in the heat map (Figure 9B). To determine the biological significance of these genes, I performed GeneSpring and IPA. However,

GeneSpring and IPA did not show any significant canonical pathway. Thus, among the differentially expressed genes, I focused on Nox1 expression because NOX1 has been reported to contribute to the maintenance of intestinal homeostasis (Lambeth and Neish, 2014).

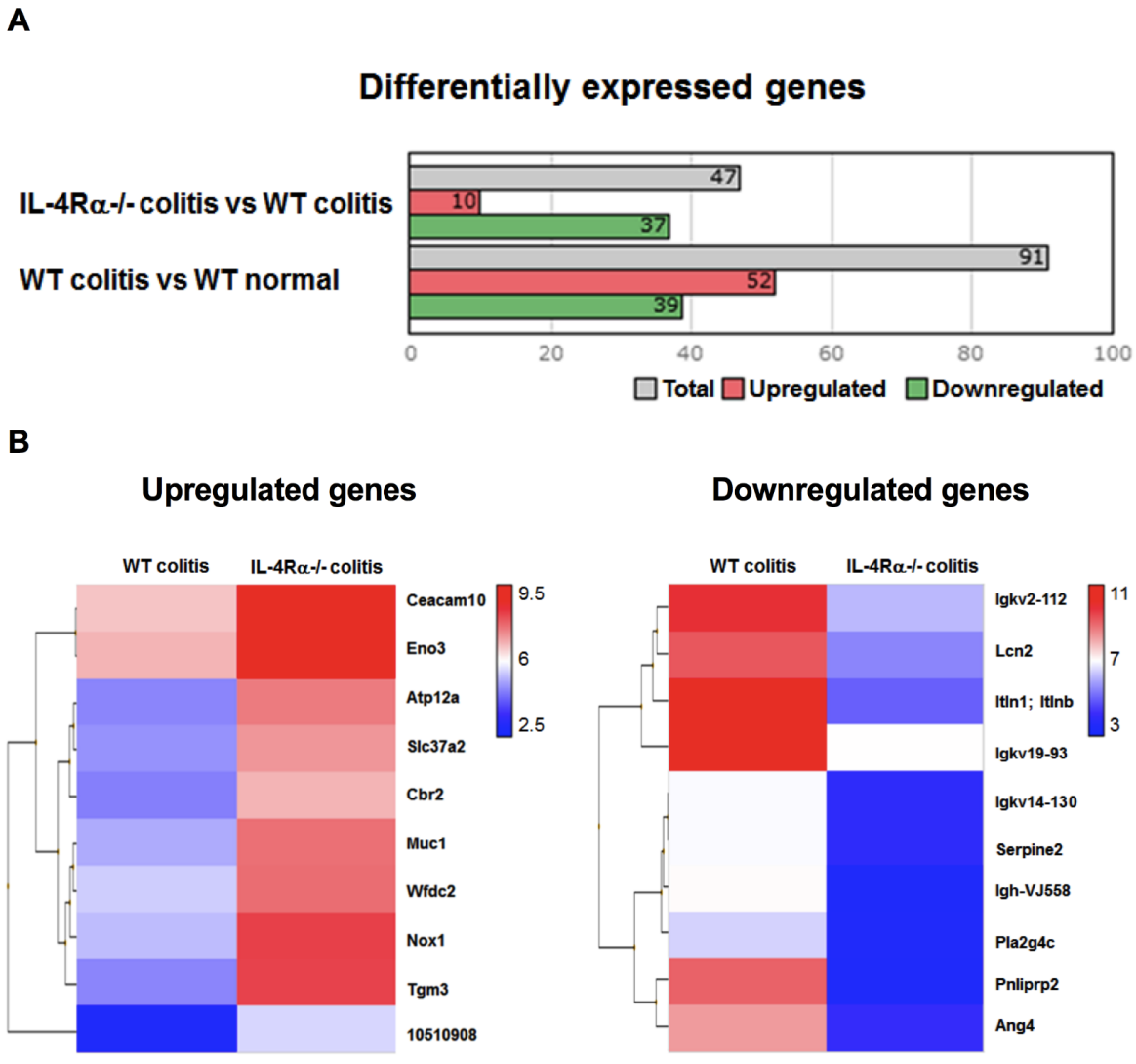

Figure 9. The transcriptomic analysis shows that IL-4Rα-/- mice exhibit a high level of Nox1 mRNA expression in the DSS-induced colitis model. Microarray data sets of WT normal, WT colitis (day 7), and IL-4Rα-/- colitis (day 7) mice are analyzed using Transcriptomic Analysis Console (TAC) Software. (A) Differentially expressed genes whose expression

levels are more than 4-fold or less than a quarter in the comparison between IL-4Rα-/- colitis and WT colitis or WT colitis and WT normal. (B) The heat map shows the top 10 upregulated (left) and downregulated (right) in IL-4Rα-/- colitis mice compared with WT colitis mice. The color range represents log2-transformed fold changes. Each row corresponds to each gene, and each column corresponds to each group. Genes were sorted using hierarchical clustering based on Euclidean distance and average linkage, as shown in the dendrogram on the left side of the heat map. The 10 gene names are displayed on the right side of the heat map.

To verify the transcriptome analysis results, I conducted qPCR to measure the mRNA expression level of *Nox1* in colitis mice. Consistent with the transcriptome analysis result, the qPCR analysis results showed that the *Nox1* mRNA expression in the colons of IL-4Rα-/- colitis mice was significantly higher than that in the colons of WT colitis mice (Figure 10A; 0.21 ± 0.04 in WT colitis, 2.00 ± 0.26 in IL-4Rα-/- colitis; $P<0.05$). Furthermore, the depletion of IL-4Rα resulted in a significant 4.2-fold increase in the mRNA expression level of *Nox1* in the colons of normal mice (Figure 10A; 0.85 ± 0.07 in WT normal, 3.53 ± 0.71 in IL-4Rα-/- normal; $P<0.05$).

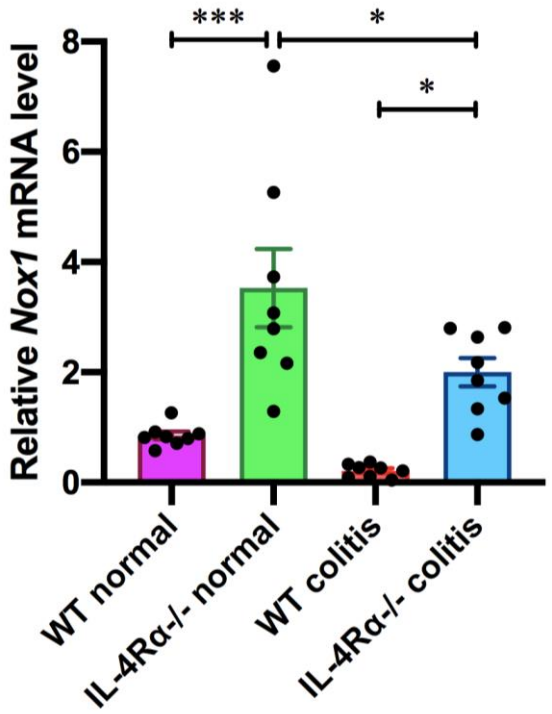

Figure 10. IL-4Rα deficiency increases NOX1-dependent ROS production in the colon of the mouse. The mRNA expression level of *Nox1* in the colons of WT and IL-4Rα-/- mice. The data are presented as the mean ± SEM values for 8 mice. *p<0.05; ***p<0.001.

To evaluate the contribution of IL-4Rα to NOX1 activity, I measured ROS production in the colonic tissues of mice. The production of ROS was significantly increased in the colons of IL-4Rα-/- normal mice compared with WT normal mice (Figure 11; $0.7x10^8 \pm 0.1x10^8$ RLU/mg protein in WT normal, $9.8x10^8 \pm 0.8x10^8$ RLU/mg protein in IL-4Rα-/- colitis; P<0.05). I also observed a significant increase in the production of ROS in the colons of IL-4Rα-/- colitis mice compared to WT colitis mice, (Figure 11; $0.8\times10^8 \pm 0.1\times10^8$ RLU/mg protein in WT colitis, $10.3\times10^8 \pm 3.2\times10^8$ RLU/mg protein in IL-4Rα-/- colitis; P<0.01). These findings indicate that IL-4Rα deficiency enhances ROS production in the colonic mucosa through the upregulation of NOX1 expression.

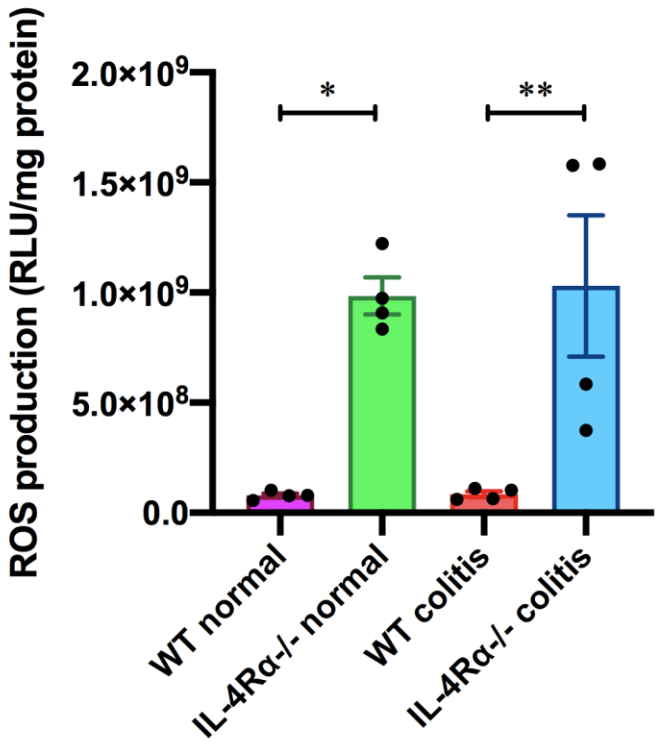

Figure 11. ROS production measurement from colon tissues samples by L-012 assay of WT and IL-4Rα-/- mice in normal and colitis condition. The data are presented as the mean ± SEM values for 4 mice and are representative of 1 of 2 independent experiments. *$p<0.05$; **$p<0.01$.

Since NOX1 expression is highly expressed in intestinal epithelial cells (Szanto et al., 2005; Valente et al., 2008), I also determined ROS production from colon epithelial cells fraction (Figure 12, n=10-12; $P<0.05$).

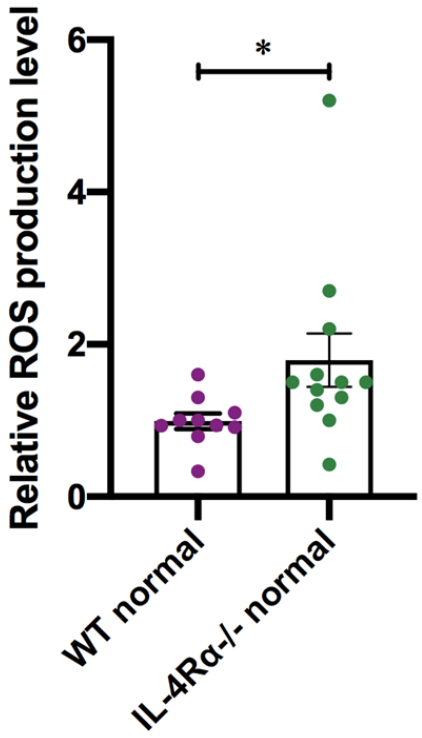

Figure 12. ROS level in the colonic epithelial fraction isolated colons of WT and IL-4Rα-/- normal mice. The data are presented as the mean ± SEM values for 10-12 mice. *p<0.05.

3.4.IL-4Rα depletion modulates intestinal barrier function in vivo

To investigate the in vivo intestinal permeability, I determined the FITC-dextran concentration in the plasma of WT and IL-4Rα-/- mice in the colon of normal and colitis mice. The FITC-dextran level was significantly suppressed in the plasma of IL-4Rα-/- colitis mice (Figure 13A; 673.9 ± 42.1 pg/ml in WT colitis; 204.0 ± 41.5 pg/ml in IL-4Rα-/- colitis; p<0.001). Interestingly, the level of plasma FITC-dextran was significantly lower in IL-4Rα-/- normal mice compared with WT normal mice (Figure 13B; 420.6 ± 93.6 pg/ml in WT normal; 177.3 ± 44.8 pg/ml in IL-4Rα-/- normal; P<0.05).

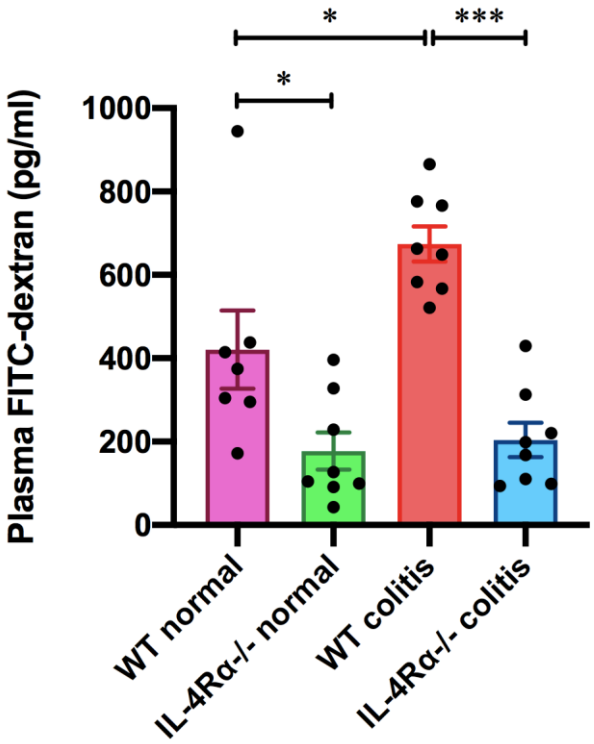

Figure 13. IL-4Rα deficiency enhances the intestinal barrier function in vivo. The concentration of FITC-dextran in the plasma of WT and IL-4Rα-/- mice are shown. Plasma samples were collected from WT and IL-4Rα-/- mice on day 0 (normal) or day 7 (colitis) after initiation of DSS treatment. The data are presented as the mean ± SEM values for 7-8 mice. *p<0.05; ***p<0.001.

In accordance with previous reports that revealed IL-4 and IL-13 play a role in the regulation of intestinal mucosal barrier function (Groschwitz & Hogan, 2009) and mediates their function through IL-4Rα, I determined the mRNA expression level of IL-4 and IL-13 in normal and colitis condition (Figure 14A; n= 4, P<0.05). The results showed, there was no difference in *Il-4* mRNA expression between WT normal and WT colitis mice. Furthermore, the depletion of IL-4Rα subunit generated 2.4-fold increase of *Il-13* mRNA expression in the colons of IL-4Rα-/- normal mice (Figure 14B, n=4, P<0.001).

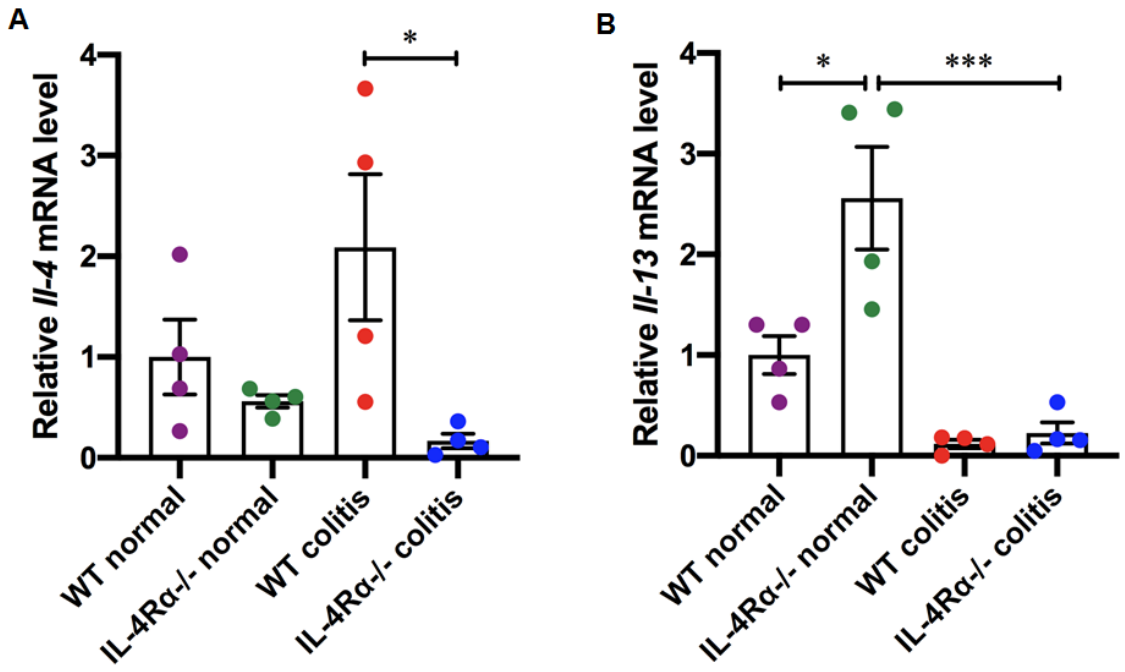

Figure 14. DSS-induced changes in the mRNA expression level of *Il-4* and *Il-13* in the colons of WT and IL-4Rα-/- mice. The data are presented as the mean ± SEM values for 4 mice. *p<0.05; **p<0.01; ***p<0.001.

4. Discussion

My recent findings indicate that the development of DSS-induced colitis is attenuated in IL-4Rα-/- mice through enhancement of NOX1-derived ROS production in the colon.

IL-4Rα-/- mice showed normal phenotypic unless challenge with worm infestation in which case they showed inability to clear the parasite and succumb to overwhelming disease burden (Herbert et al., 2004). IL-4Rα-/- mice experienced loss of IL-4 signal transduction and functional activity and exhibited lack sensitivity to IL-4 stimulation (Noben-trauth et al., 1997).

IBD is a chronic inflammatory disorder attack the gut, which comprise of Crohn's disease and UC (Maloy and Powrie, 2011; Kaser et al., 2010). Genetic, clinical, and experimental studies have shown that IBD is a multifactorial disease in which a genetically inadequate host

response to environmental factors leads to a breakdown of the intestinal mucosal barrier (Maloy and Powrie, 2011). Maintenance of the intestinal mucosal barrier is mediated by a tissue-specialized cellular network via the signaling pathways of various cytokine receptors (Friedrich et al., 2019). The disintegration of the cellular network regulated by cytokines and their receptors is recognized as the pathogenic mechanism underlying disorders of chronic intestinal inflammation, such as IBD. Indeed, many IBD risk loci have been found in regions of genes encoding cytokines or their downstream signaling mediators (Liu et al., 2015). An IL-13-dependent abnormal Th2 cell response has been observed in the colonic mucosa of IBD patients (Heller et al., 2005). IL-4 and IL-13 have also been reported to play critical pathogenic roles in animal models of colitis (Mizoguchi et al., 1999; Heller et al., 2002). IL-4Rα was strongly expressed in the colonic tumors of murine colitis-associated cancer (CAC) model in WT mice, and the number and size of colonic tumors were significantly reduced in IL-4Rα-/- CAC mice through the suppression of epithelial tumor proliferation due to lack of IL-4Rα-/- signaling, however, there was no information about the inflammation in this previous study (Koller et al., 2010). Although the involvement of IL-4Rα in the disruption of epithelial barrier function in IBD patients has been suggested (Heller et al., 2005), no direct evidence has revealed the role of IL-4Rα in mediating intestinal inflammation.

To investigate the contribution of IL-4Rα in the intestinal mucosal inflammation, I used experimental acute colitis using DSS as an inducing agent. Mice deficient in IL-4Rα exhibited obvious amelioration of symptoms of DSS-induced colitis such as diarrhea, rectal bleeding, colon shortening, and destruction of the colonic mucosal structure. In addition, DSS-induced neutrophil infiltration in the colonic mucosa was decreased in IL-4Rα-/- mice. Neutrophil infiltration in the mucosa is mediated by specific chemoattractant such as CXCL1, CXCL2 (also known as macrophage inflammatory protein 2; MIP2) and CXCL8 (Farooq et al, 2009). Notably, CXCL2-overexpressing transgenic mice showed that the increased number of MPO-positive neutrophils in the colonic lamina propria of normal and DSS-treated mice (Ohtsuka and Sanderson, 2003). Intestinal mucosal neutrophils, which infiltrate the inflamed mucosa of IBD patients and animals in experimental colitis models, produce various cytokines that trigger further inflammatory responses (Baumgart and Carding, 2007).

Among these cytokines, IL-1β exhibits increased production in the model of DSS-induced colitis (Melgar et al., 2005; Hayashi et al., 2017). We previously reported that the expression level of IL-1β in the colonic mucosa was positively correlated with the disease severity of DSS-induced colitis in mice (Hayashi et al., 2017). Furthermore, IL-1β secreted from infiltrated neutrophils in the colonic mucosa contributes to the pathogenesis of colitis (Wang et al., 2014). In the present study, the infiltration of neutrophils and the upregulation of CXCL2 and IL-1β observed in colonic tissues of colitis mice were significantly suppressed in the IL-4Rα-/- mice. These findings strongly demonstrate that IL-4Rα-/- mice exhibit reduced susceptibility to inflammatory responses in the intestine.

Since IL-4 and IL-13 have been reported to play the role in intestinal mucosal barrier function (Grocshwitz and Hogan, 2009) I also measured *Il-4* and *Il-13* mRNA expression in the colonic tissues of normal and colitis mice (Figure 14). The mRNA expression of *Il-4* was significantly lower in IL-4Rα-/- colitis mice than in WT colitis mice. IL-4 deficient mice have been reported to show amelioration of the DSS-induced colitis (Stevceva et al., 2001), suggesting the pathogenic role of IL-4 in DSS-induced colitis model. However, the roles of IL-4 in the DSS-induced colitis model are still controversial because protective roles of IL-4 have been also reported (Kim and Chung, 2013). In the present study, there was no difference in *Il-4* mRNA expression between WT normal mice and WT colitis mice. Furthermore, the depletion of IL-4Rα resulted in a 2.4-fold increase in the mRNA expression level of *Il-13* in the colons of IL-4Rα-/- normal mice. Since IL-13 increases intestinal permeability dependent on IL-4Rα/STAT6 activation elevated IL-13 in IL-4Rα-/- normal mice is assumed to not affect intestinal permeability due to lack of IL-4Rα in the present study. Although IL-4 and IL-13 are recognized as key cytokines for IL-4Rα-mediated mucosal barrier function (Groschwitz and Hogan, 2009), further detailed studies are required to understand the role of IL-4 and IL-13 in the intestinal mucosal barrier function in vivo.

My recent study revealed that colonic tissues of IL-4Rα-/- mice give high *Nox1* mRNA expression levels under both steady-state and inflammatory conditions. According to the previous study, NOX1 is NADPH oxidase and is a major source of ROS in nonphagocytic cells (Lambeth and Neish, 2014). This study also reported that NOX1-dependent ROS

production in the intestinal epithelial cells plays a crucial role in intestinal homeostasis maintenance (Lambeth and Neish, 2014). Impaired ROS production due to Nox1 gene mutation has been suggested to be associated with an increased risk of very early onset IBD (Hayes et al., 2015; Stenke et al., 2019). IL-10 deficient mice are well known as a model of spontaneous colitis (Kühn et al., 1993) because IL-10 produced from intestinal macrophages plays an important role in the regulation of intestinal homeostasis during host defense mechanism (Maloy and Powrie, 2011; Hayashi, 2020). Double-deficient Nox1 and IL-10 mice showed earlier colitis symptoms compared with IL-10-deficient mice (Tréton et al., 2014). In addition, mutant mice that produce a low level of intestinal ROS developed more severe DSS-induced colitis compared with WT mice (Aviello et al., 2019). In this present study, I found that IL-4Rα depletion elevated the production of ROS in colonic tissues of normal mice. These findings indicate that IL-4Rα depletion in mice enhances ROS generation due to the upregulation of Nox1 expression in the colon, and lead to colitis severity attenuation.

However, the pathogenic roles of NOX1-derived ROS in colitis have also been reported. Administration of apocynin, an antioxidant and a nonselective NADPH inhibitor, suppressed the inflammatory response in a model of DSS- and tumor necrosis factor-α-induced colitis(Mouzaoui S et al., 2014; Ramonaite R et al., 2014). NOX1-deficient mice exhibited reduced susceptibility to trinitrobenzene sulfonic acid-induced colitis by suppressed proinflammatory cytokine expression in the macrophages (Yokota et al., 2017; Makhezer et al; 2019). These contradictory results in the colitis model using NOX1-deficient mice may be due to the differences in the colitis models and the responsible cells in which NOX1 functions.

Several reports showed that since NOX1 is highly expressed in intestinal epithelial cells (Szanto et al., 2005; Valente et al., 2008), epithelial NOX1-derived ROS have been reported to play an important role in the regulation of intestinal epithelial integrity. My current results showed the ROS production from colon epithelial fraction of IL-4Rα-/- was 1.8-fold higher compared with WT colon epithelial cell fraction. But the ROS measurement from colon epithelial cell fraction exhibited lower ROS production than colon tissue sample ROS. I

thought probably ROS production may not measure accurately using this method. I have to consider another protocol to determine ROS production from colon epithelial fraction, for example by utilize organoid techniques. ROS measurement from colon epithelial cells organoid have been reported in several research (Levy et al., 2020; Moll et al., 2018; Cheung et al., 2015).

Intestinal epithelial NOX1-derived ROS generation and subsequent ROS signaling have been demonstrated to control intestinal mucosal wound repair after injury (Leony et al., 2013). ROS generated by epithelial NOX1 was involved in the proliferation and differentiation of colonic epithelial cells by modulating the PI3K/AKT/Wnt and Notch signaling pathways (Coant et al., 2010). In addition, NOX1-mediated cellular ROS production was also required for collective migration of epithelial cells, because defective directional migration and altered cell-cell contact were observed in cells with loss of NOX1 function (Khoshnevisan et al., 2020). Intestinal epithelial cells cover the outermost surface of the mucosa and interface with the lamina propria to form the intestinal mucosal barrier (Quiros and Nusrat, 2019). Thus, NOX1-dependent ROS production in the intestinal epithelial cells is considered an important property for intestinal barrier integrity maintenance. These findings led to the hypothesis that IL-4Rα mediates intestinal mucosal barrier function via regulation of NOX1-dependent ROS production. To address this hypothesis, I investigate intestinal barrier function in IL-4Rα-/- mice which is assessed by the intestinal permeability approach, because intestinal permeability is important functional feature of intestinal mucosal barrier function (Luissint et al., 2016; Wilms et al., 2020). IL-4Rα-/- mice exhibited a reduction of intestinal permeability to 4 kDa FITC-dextran, indicated that the intestinal barrier function of IL-4Rα-/- mice might be strengthened by enhancement of Nox1-derived ROS production. However, further studies are needed to clarify the mechanism by which IL-4Rα signaling regulates NOX1 expression in intestinal epithelial cells.

Given the findings of my present study, I conclude that IL-4Rα deficiency enhances NOX1-dependent ROS production and intestinal mucosal barrier function, resulting in the suppression of colitis development (Figure 15). The mechanism of how IL-4Rα signaling

could regulate the NOX1-dependent ROS production remain elusive because almost all of previous report related to redox regulation by IL-4 signaling required IL-4Rα (Sharma et al., 2008; Liu H et al., 2017).

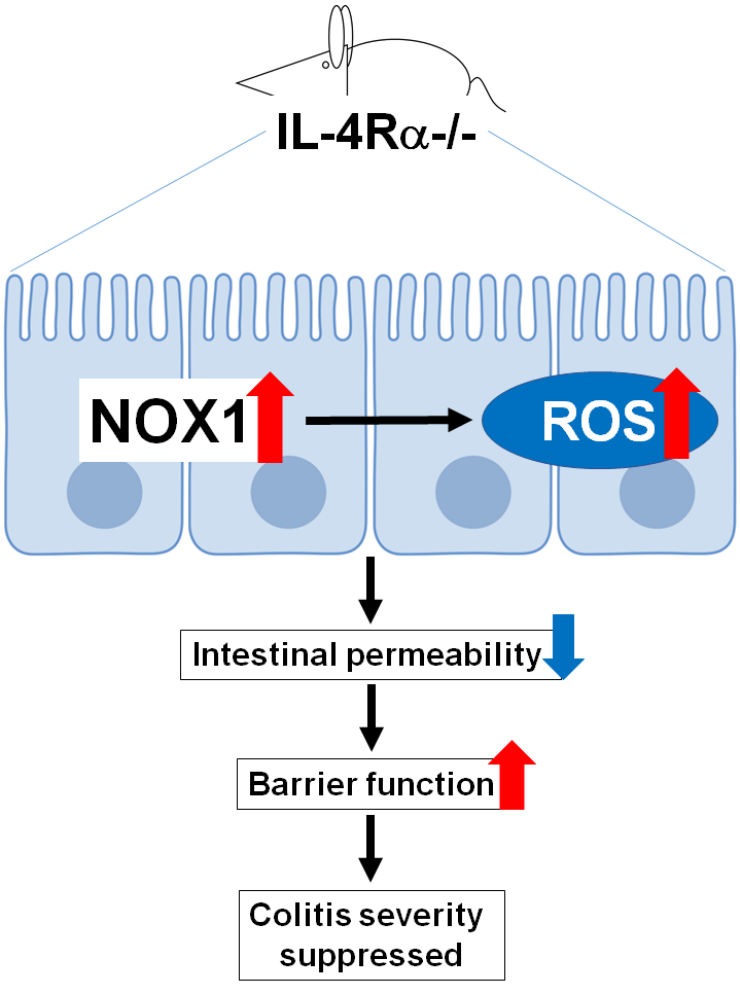

Figure 15. Schematic representation of how depletion of IL-4Rα subunit alleviates intestinal inflammation in IL-4Rα-/- colitis mice through enhancement of NOX1-dependent ROS production that strengthens intestinal permeability.

Chapter 2

Morphological investigation of GPR41-positive enteric sensory neurons in the colon of mice with DSS-induced colitis

1. Introduction

Inflammatory bowel disease (IBD) is a chronic relapsing disease of the gastrointestinal tract that includes ulcerative colitis (UC) and Crohn's disease (CD). Although the etiology of IBD remains unclear, it has generally been accepted that abnormalities of the intestinal immune system and dysbiosis of the gut microbiota are involved in the pathogenesis of IBD.

The gut microbiota is a pivotal contributor to human health. Some of its effects are at least partly mediated by short-chain fatty acids (SCFAs), consisting mainly of acetate, propionate, and butyrate produced by the microbiota. Dysbiosis is defined as an alteration in the gut microbiota composition that results in an imbalance between beneficial and harmful bacteria (Machiels et al., 2014; Nishida et al., 2018). Indeed, dysbiosis is associated with predisposition to numerous human diseases, including non-gastrointestinal diseases, such as diabetes and Alzheimer's disease. Genome-wide association studies have revealed that more than 200 genes associated with susceptibility to IBD are involved in mediating the host response to the gut microbiota (Nishida et al., 2018).

Recently, SCFAs have been shown to regulate the functions of intestinal immune cells through the activation of SCFA-sensing G protein-coupled receptors (GPCRs), such as GPR41 and GPR43 (Kimura et al., 2020). GPR41 and GPR43 are thought to at least partially mediate the interaction between the host and the gut microbiota (Ang and Ding, 2016). It has also been reported that GPR41 and GPR43 are colocalized in enteroendocrine cells as sensors for SCFAs in GPR41-mRFP and GPR43-mRFP transgenic mice (Nøhr et al., 2013). GPR41 also reported to expressed in cell bodies of enteric neurons but cannot be detected in nerve fibers of mucosa and enteric ganglia (Nøhr et al., 2013). However, there is no information available concerning which type of enteric neuron GPR41 is located. To date, there have

been several studies on the pathological roles of GPR41 and GPR43 in chronic inflammatory disorders such as colitis, asthma, and arthritis using knockout mice (Kimura et al., 2020). However, studies have shown conflicting evidence as to whether GPR41 and GPR43 are protective or causative, and many questions regarding the functions of GPR41 and GPR43 remain unanswered (Ang and Ding, 2016).

The DSS-induced acute colitis model is the most widely used animal model of IBD and causes dysbiosis, which is usually experienced in IBD patients (Munyaka et al., 2016). In DSS-induced colitis, intestinal macrophages in the inflamed colonic mucosa respond to microbial stimulation and produce large amounts of proinflammatory cytokines. These proinflammatory cytokines will lead to the destruction of the colons (Platt et al., 2010). Our previous report has been revealed that the proportion of F4/80-positive macrophages were increased in the mouse colon in response to DSS treatment (Hayashi et al., 2017). However, DSS-induced colitis studies related to dysbiosis have rarely been carried out.

Therefore, to determine pathophysiological roles of GPR41 in the intestinal inflammation, I conducted morphological characterization of GPR41, enteric nerve fibers, and F4/80-positive macrophages in the colonic mucosa of DSS induced colitis mice.

2. Materials and Methods

2.1.Animal

Male BALB/c mice aged 8 weeks and male C57BL/6 mice aged 10-12 weeks were purchased from SLC (Shizuoka, Japan). Mice were housed in a room with a light/dark cycle (12 h: 12 h) in the experimental animal facility at University of Toyama and were provided free access to food and water. All of the animal care procedures and experiments were approved by the Animal Experiment Committee at the University of Toyama (authorization No. A2018 INM-3).

2.2.DSS-induced colitis model

BALB/c mice were treated with 3% DSS (36-50 kDa; MP Biomedicals, Santa Ana, USA) in the drinking water for 7 days (Hayashi et al., 2017). Assessments of colitis severity were made by daily observation of body weight, stool consistency, and the presence of blood in the stool. The disease activity index was calculated as the average of 2 parameters: diarrhea (0, normal; 1, soft stool; 2, loose stool; 3, mild diarrhea; 4, severe diarrhea) and blood in the stool (0, normal; 1 faint bleeding; 2, slight bleeding; 3 gross bleeding; 4, severe bleeding). Whole colons were excised on day 7 after DSS administration. The assay was terminated when weight loss reached 20% of initial body weight as the humane endpoint.

2.3.Determination of proinflammatory mRNA expression

Proinflammatory mRNA expression was determined in the excised distal colon as described previously (Hayashi et al., 2017). Briefly, total RNA was extracted from the colon tissue using Sepasol RNA I Super (Nacalai Tesque, Kyoto, Japan) according to the manufacturer's instructions. Reverse transcription was carried out using the PrimeScript RT Reagen Kit (Takara Bio, Ohtsu, Japan). Real-time PCR amplification of *Il-1β*, *Il-6*, and *Gapdh* was performed using TB Green Premix EX Taq (Takara Bio, Ohtsu, Japan). The levels of target mRNAs were normalized to those of *Gapdh* as an internal control for each sample. The primer sequences are shown in Table 1.

2.4.Histological analysis

Histological analysis was performed in accordance with previous experiments (Hayashi et al., 2014). Briefly, the distal colon was removed, washed in ice-cold phosphate-buffered saline, and fixed in 4% paraformaldehyde for 24 h at 4°C. After treatment with 30% sucrose solution, the tissue sample was embedded in Tissue Freezing Medium (TBS, Durham, NC, USA), and sliced 10 μm thickness at -20°C using cryostat microtome (Leica Microsystems, Nussloch, Germany). The sections were then routinely stained with H&E and scored for inflammation and crypt damage as described previously (Hayashi et al., 2014).

2.5.Antibiotic-induced gut dysbiosis model (ABX model)

Antibiotic-induced gut dysbiosis model was performed based on the previous report (Hill et al., 2010). Briefly, C57BL/6 mice received an antibiotic cocktail which comprised of ampicillin (1 mg/ml), vancomycin (0.5 mg/ml), metronidazole (1 mg/ml), and neomycin (1 mg/ml by oral gavage for 10 days. Mice were sacrificed on day 10 after antibiotic treatment. Each cecum was carefully dissected and weighed.

2.6.Immunohistochemical analysis

Immunohistochemistry was performed according to the procedure described in previous reports (Lee et al., 2013). Briefly, the excised distal colons were fixed with 4% paraformaldehyde for 24 h at 4 ℃. After treatment with a 30% sucrose solution, the tissue sample was embedded in OCT compound (Sakura Finetek, Tokyo, Japan). The frozen sections (30 μm) were exposed to a rabbit anti-human GPR41 antibody (ab236654, Abcam, Cambridge, USA), goat anti-rat CGRP antibody (ab36001, Abcam), or rat anti-mouse F4/80 (MCA497GA, BioRad, Hercules, CA) for 12−18 h at 4°C and then incubated with the appropriate secondary antibodies for 2 h (Alexa 488 donkey anti-rabbit IgG, Cy3 donkey anti-rabbit IgG, Cy3 donkey anti-goat IgG or Alexa 488 donkey anti-rat IgG (Jackson ImmunoResearch Laboratories)) at room temperatures. The immunostained sections were examined using a confocal microscope (LSM700 & LSM780). To avoid selection bias, three representative preparations were selected from each mouse colon and then three mucosal sites of each preparation were quantitatively analyzed using open-source software imageJ (NIH, Bethesda, MD, USA).

2.7.Statistical analysis

All data are presented as the mean ± SEM. Statistical analyses were performed using an unpaired Student's t-test. Probability (P) values <0.05 were considered statistically significant.

3. Results

3.1. DSS-induced colitis model

To generate dysbiosis conditions related to IBD, I used 3% DSS to induced the acute colitis model in BALB/c mice. In the colitis mice, body weight loss, diarrhea, and blood in the stool first appeared on day 4 after DSS treatment started. Significant body weight loss was observed on day 7 in the colitis mice (Figure 16A. 78.7 ± 1.9% of initial body weight in colitis mice; 102.4 ± 1.0% of initial body weight in normal mice, n=7, $P<0.01$). The DAI score of colitis mice also showed a significant difference compared to those of normal mice (Figure 16B; 3.4 ± 0.2, n=7, $P<0.01$). Macroscopic observations showed colon shortened in colitis mice caused by DSS treatments (Figure 16C; 7.9 ± 0.2 cm in colitis mice vs 11.9 ± 0.4 cm in normal mice, n=7, $P<0.01$).

The mRNA expression level of *Il-1β* and *Il-6* on day 7 was markedly upregulated in the colon of colitis mice compared with normal mice (Figure 17A. *Il-1β*: colitis mice: 17.4 ± 5.4, normal mice: 1.0 ± 0.3, n=7, $P<0.05$; Figure 17B. *Il-6*: colitis mice: 377.6 ± 164.2, normal mice: 1.0 ± 0.6, n=7, $P<0.05$). Destruction of epithelial integrity and crypt architecture was observed on day 7 in the colons of colitis mice.

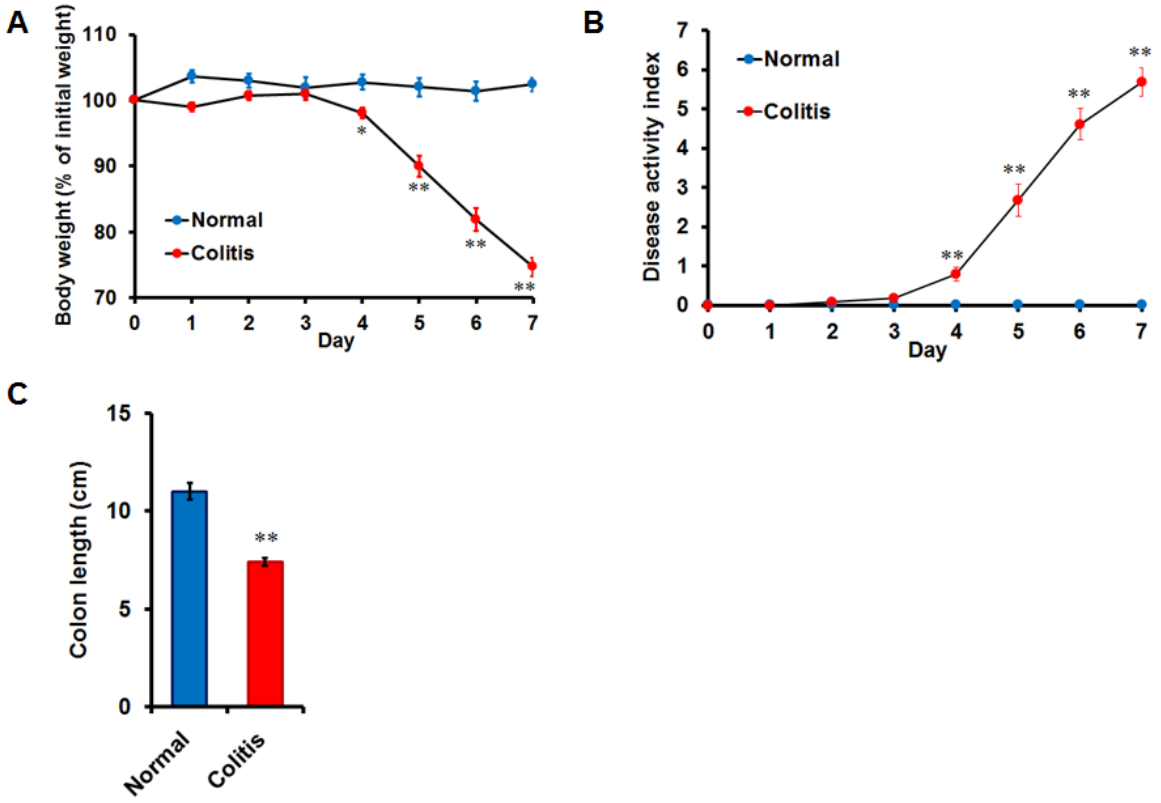

Figure 16. Treatment with 3% DSS in BALB/c mice for 7 days (A) induced body weight loss, (B) increase the disease activity index (diarrhea and blood in the stool; DAI score), (C) shortened the colon. The data are presented as the mean ± SEM of 7 mice, * $p<0.05$, and ** $p<0.01$ compared with normal mice by Student's t-test.

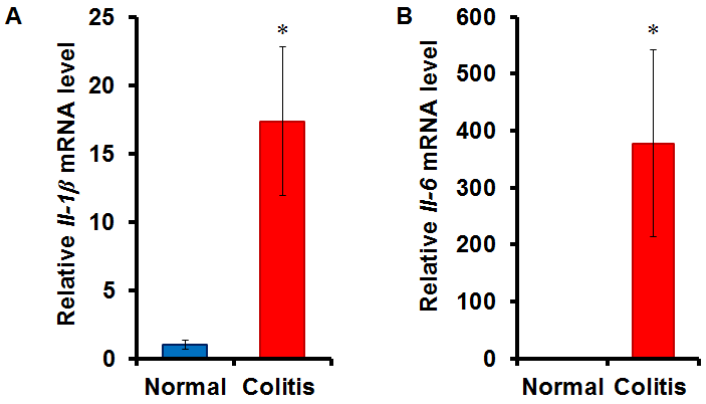

Figure 17. The changes in the mRNA expression of proinflammatory mediators *Il-1β* and *Il-6* induced by DSS treatment in the colon of normal and colitis mice. (A) The relative mRNA expression level of *Il-1β*, and (B) relative mRNA expression level of *Il-6*. The data are presented as the mean ± SEM of 7 mice; *p<0.05 compared with normal mice by Student's t-test.

3.2. GPR41 expression was markedly increased in the colon of colitis group

GPR41-IRs were observed in the nerve-like fibrous structures (Figure 18A: arrowheads) of both lamina propria and muscularis layer and in the cell somas of enteric neurons (Figure 18A: arrow). This result was indicated that GPR41 is expressed in both nerve fibers and cell somas of enteric neurons, especially myenteric neurons. Moreover, GPR41-IRs were significantly increased in the colonic lamina propria of the colitis group approximately 2-fold in the colonic lamina propria of colitis mice compared with normal mice (Figure 18B, n=5, P<0.01)

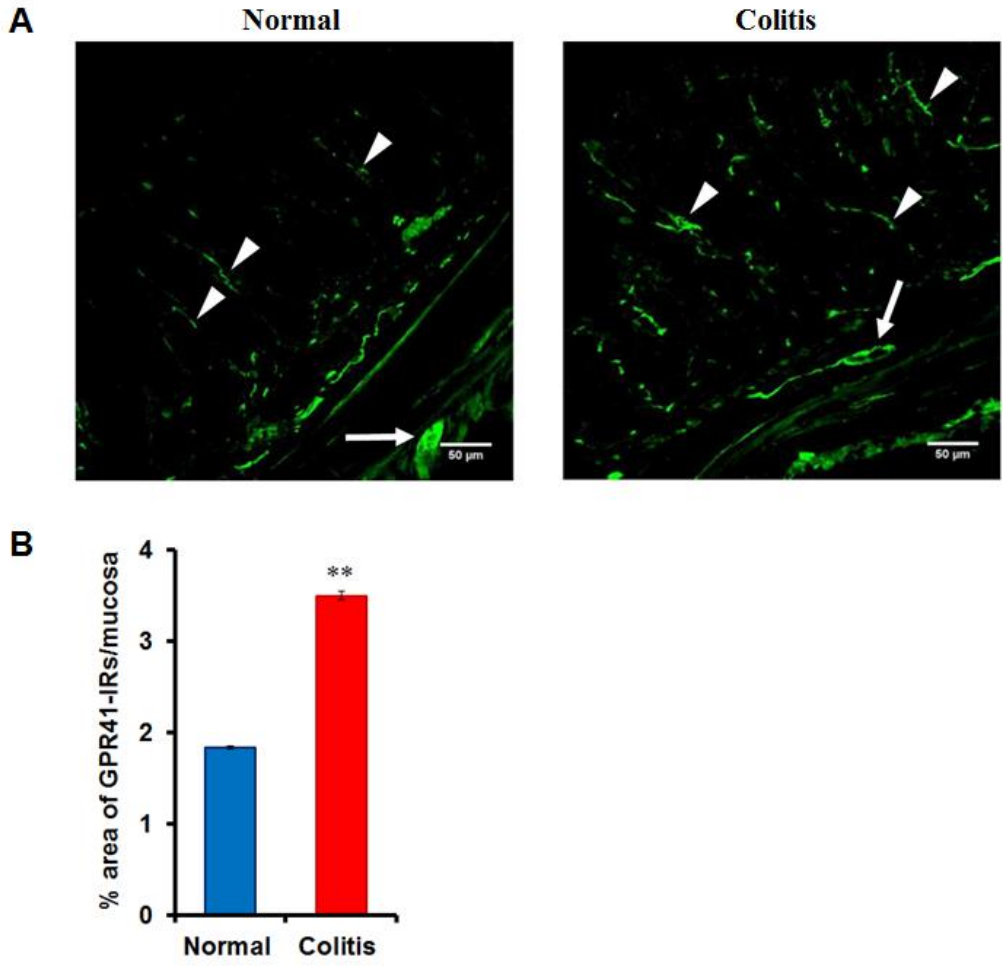

Figure 18. GPR41 immunoreactivities in the colon of normal and colitis mice. (A) Representative images of GPR41-IRs in the colons of normal and colitis mice, (B) quantitative analysis of GPR41-IRs in the lamina propria of the mouse colon. Arrowhead: nerve fibers; arrow: neurons. The data are presented as the mean ± SEM of 5 mice, **p< 0.01 compared with normal mice by Student's t-test.

3.2.CGRP expression was significantly increased in the colon of colitis group

Our recent study reveals that CGRP-IRs were observed in nerve fibers of the colonic lamina propria (Figure 19A: arrowheads) and enteric neurons (Figure 19A: arrow) of mice colon (Figure 19A). Quantitative analysis was showed that CGRP expression in the colonic

lamina propria of the colitis group was significantly increased by 41.4 ± 8.9% compared with the normal group (Figure 19B, n=5, P<0.01).

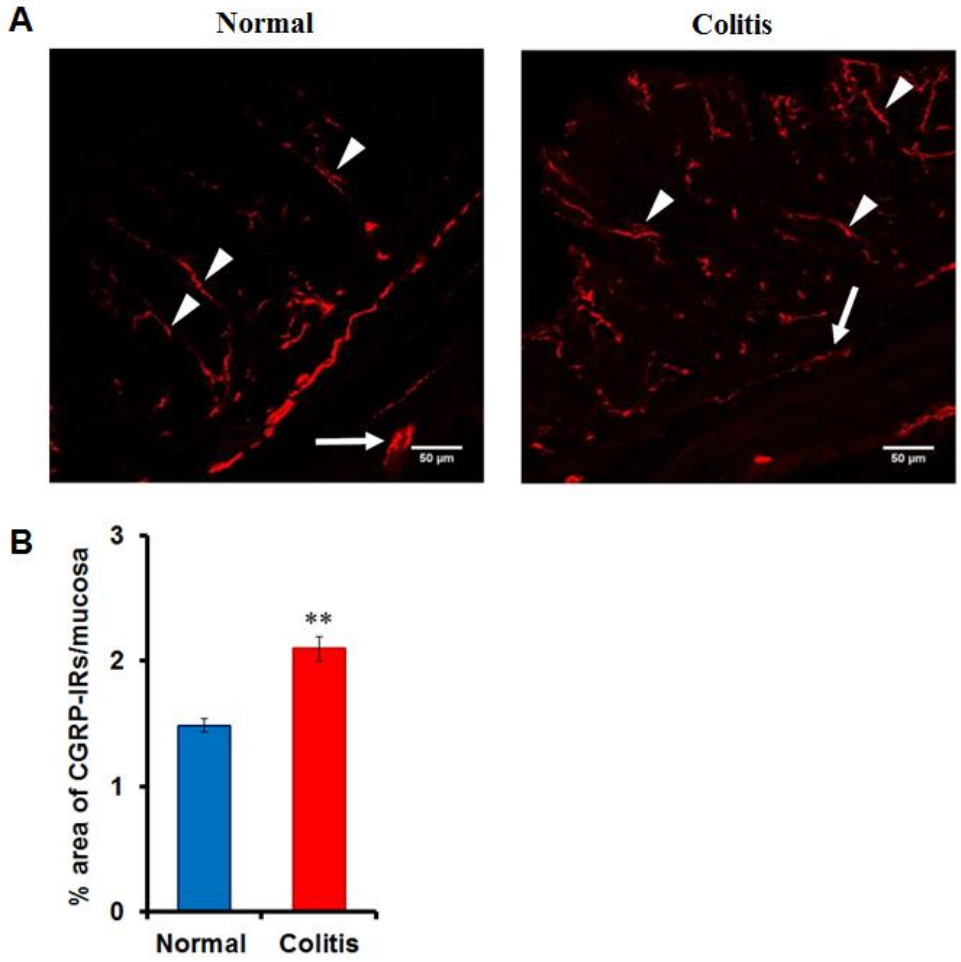

Figure 19. 3% DSS treatment for 7 days elevated CGRP-immunoreactivities in mouse colonic mucosa. (A) Representative images of CGRP-IRs in mice colonic mucosa in normal and colitis condition. (B) Quantitative analysis of CGRP-IRs in the lamina propria of the mouse colon of normal and colitis mice. Arrowhead: nerve fibers; arrow: neurons. The data are presented as the mean ± SEM of 5 mice, **p<0.01 compared with normal mice by Student's t-test.

3.3.Colocalization of GPR41 and CGRP was observed in the colonic lamina propria of colitis group

GPR41-IRs are partly colocalized with CGRP-IRs in the colonic lamina propria and muscularis layer of normal and colitis mice (Figure 20A), indicating that GPR41 is located in the nerve fibers and cell somas of cholinergic intrinsic sensory neurons in the mouse colon.

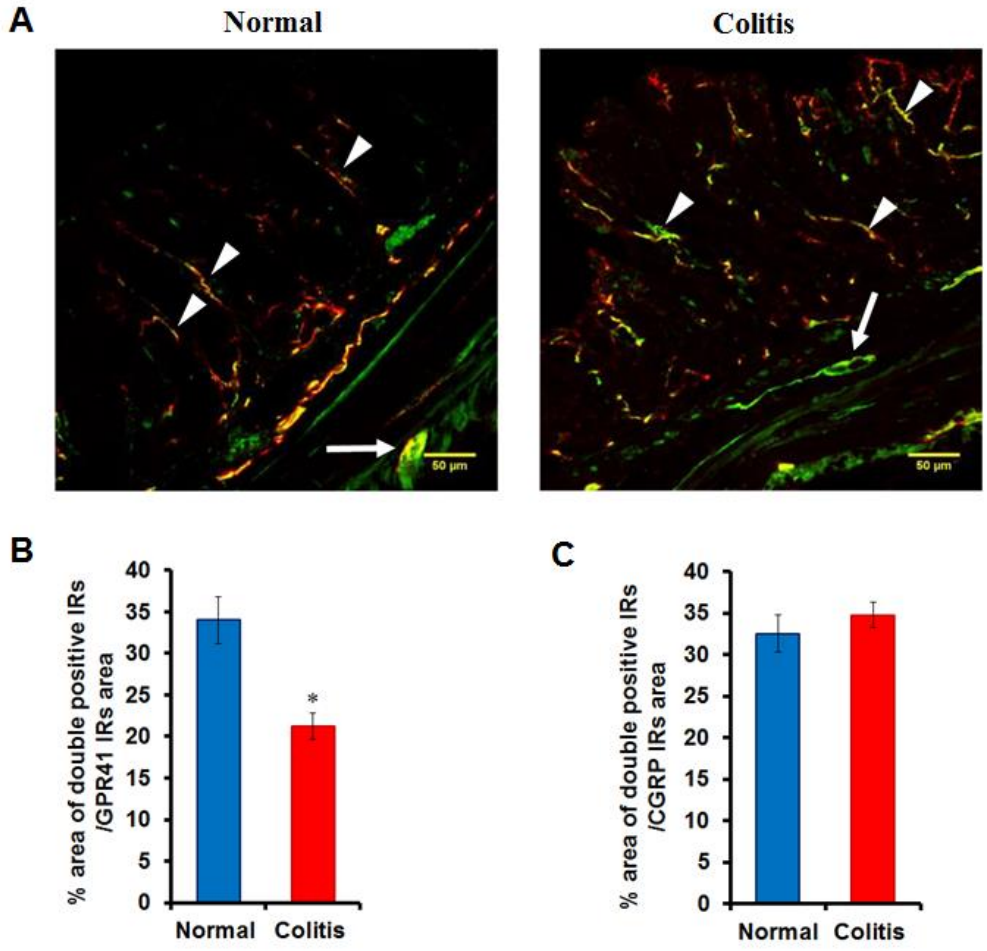

Figure 20. GPR41-IRs are partly colocalized with CGRP-IRs in the colonic lamina and muscularis layer of normal and colitis mice. (A) Representative images of double-positive IRs of GPR41 and CGRP in the colonic lamina propria and muscularis layer of mice colon after DSS treatment for 7 days. Arrowhead: nerve fibers; arrow: neurons. (B) Quantitative analysis of double-positive IRs/GPR41 IRs area. (C) Quantitative analysis of double-positive

IRs/CGRP IRs area. The data are presented as the mean ± SEM of 5 mice, *p<0.05 compared with normal mice by Student's t-test.

The ratio of double-positive IRs to GPR41-IRs in the colonic lamina propria was significantly reduced in mice with colitis (Figure 20B; colitis mice: 21.2 ± 1.6%; normal mice: 34.0 ± 2.8%, n= 5, P<0.05). On the other hand, the ratio of double-positive IR to CGRP-IRs was not affected by colitis treatment (Figure 20C).

3.4. GPR41 and F4/80 immunoreactivity in DSS-induced acute colitis model showed morphological interaction between macrophages and GPR41-positive nerve fibers

To determine whether GPR41 involvement in the pathology of intestinal inflammation related to neuro-immune interaction I performed immunohistochemistry against GPR41 and F4/80 antibody. My research found that intestinal F4/80-positive macrophages were located in the colonic lamina propria colitis mice (Figure 21A). The proportion of F4/80-positive macrophages was increased in the colitis group after DSS treatment compared with normal mice (Figure 21B, n=3, P<0.01). GPR41-immunoreactive nerve fibers were found in the colonic lamina propria of the colitis mice (Figure 21A), which many of them were juxtaposed with F4/80-positive macrophages (Figure 21A). The number of F4/80-positive macrophages in close proximity to GPR41-positive nerve fibers were increased in the colonic lamina propria of colitis mice (Figure 22A, B, n= 3, P<0.05).

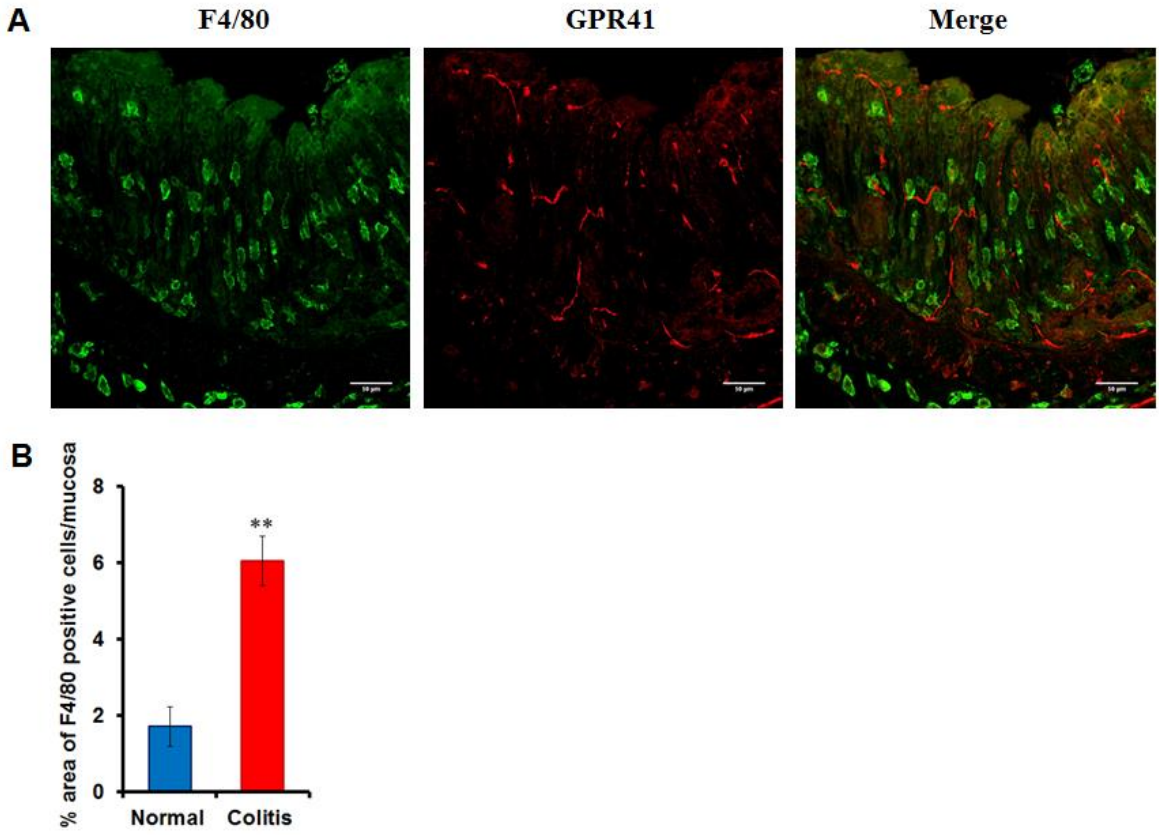

Figure 21. Morphological proximity between GPR41-positive nerve fibers and F4/80-positive macrophages in the colon of mice with DSS-induced colitis. Treatment with 3% DSS increased GPR41-IRs and F4/80-IRs in the colon of mice with colitis. (A) representative images of F4/80-positive macrophages in the colon of colitis mice, (B) quantitative analysis of F4/80-positive macrophages in the colon of normal vs colitis mice, (C) representative images of GPR41-positive nerve fibers in the colon of colitis mice, and (D) representative images of the morphological proximity between GPR41-positive nerve fibers and F4/80-positive macrophages in the colon of colitis mice. The data are presented as the mean ± SE of 3 mice, **$p<0.01$ compared with normal mice by Student's t-test.

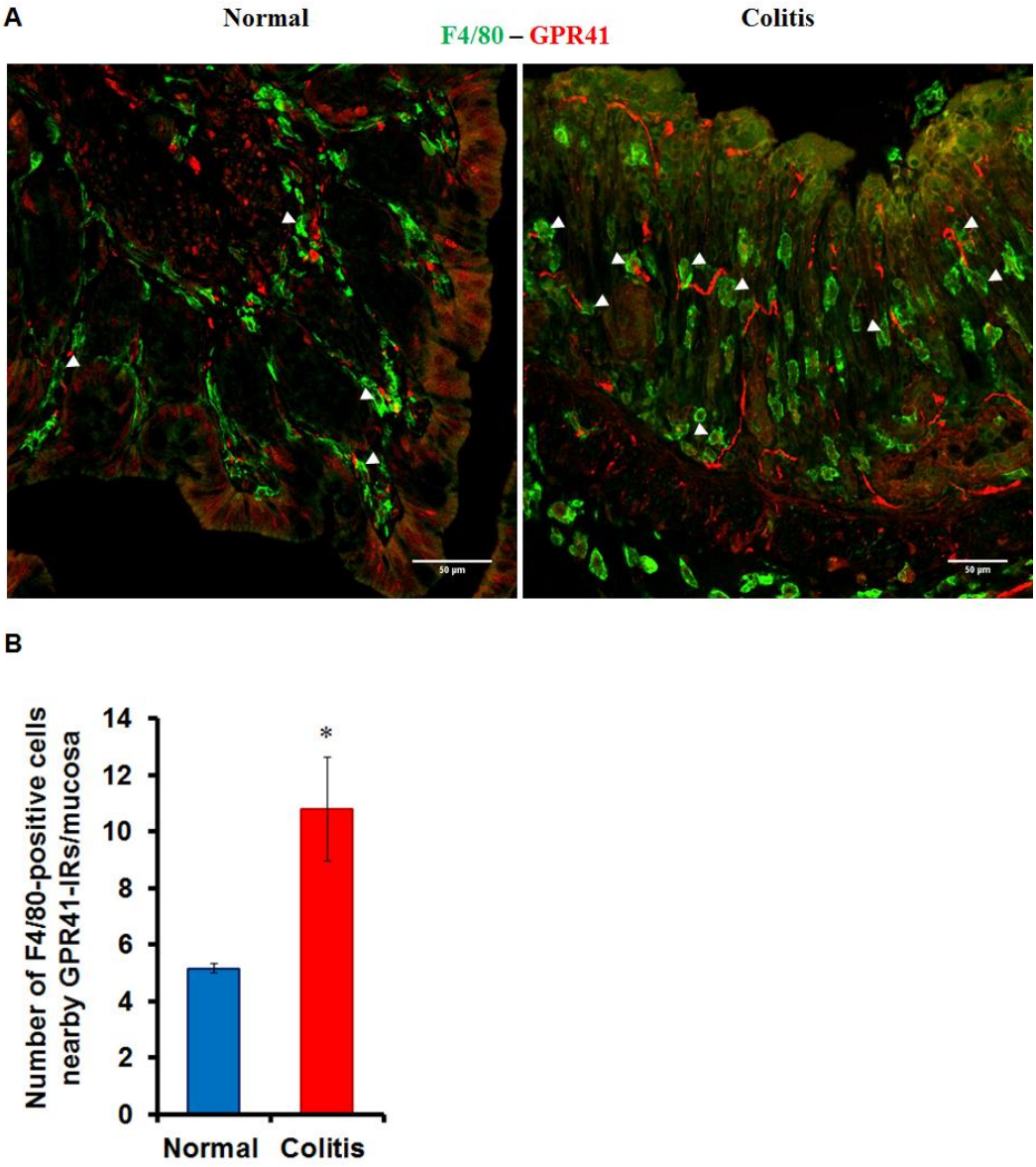

Figure 22. The number of F4/80-positive macrophages in close proximity to GPR41-positive nerve fibers were increased in the colonic lamina propria of colitis mice (A) Representative images of F4/80-positive macrophages in close proximity to GPR41-positive nerve fibers in the colonic lamina propria of normal and colitis mice. (B) Histogram showed the number of F4/80-positive macrophages in close proximity to GPR41-positive nerve fibers. The data are presented as the mean ± SE of 3 mice, *$p<0.05$ compared with normal mice by Student's t-test.

3.5.GPR41 and CGRP immunoreactivities in the mice colonic mucosa after antibiotic treatment for 10 days

Antibiotic cocktail treatment for 10 days showed markedly increased the size of mouse cecum (Figure 23A and 23B; 712.86 ± 50.46 mg in ABX-treated mice; 378.57 ± 16.82 mg in vehicle-treated mice; n=7, P<0.01). This result suggested that dysbiosis of the gut microbiota occurred after 10 days of antibiotic treatments.

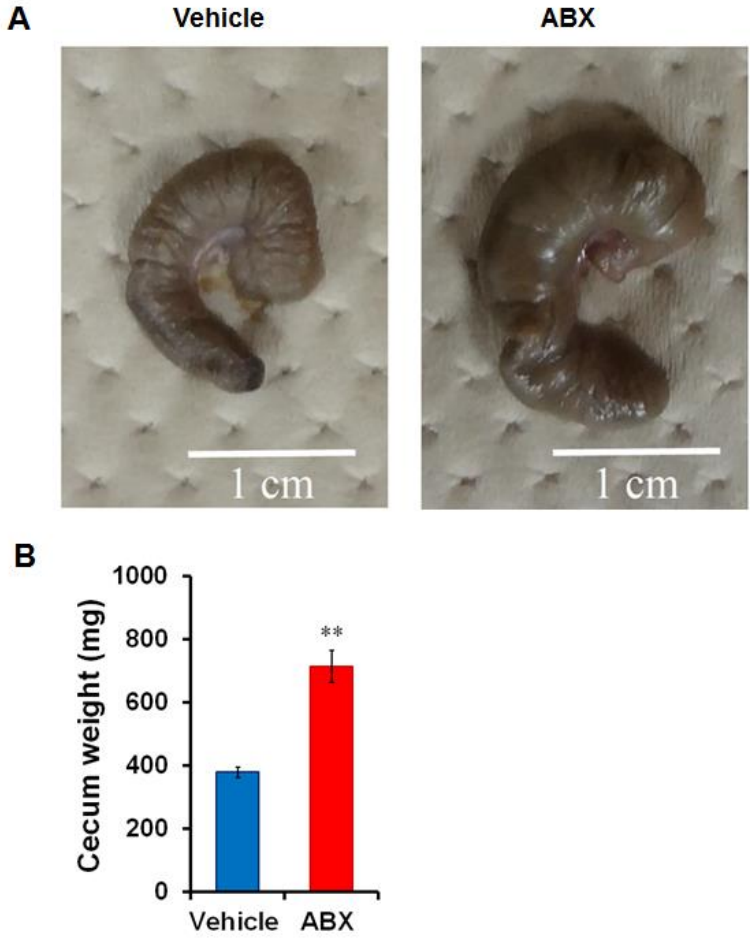

Figure 23. Antibiotic treatment for 10 days induced gut dysbiosis in mice shown by cecum enlargement. (A) Representative images of mice cecum of vehicle and ABX mice. (B) Cecum weight comparison between vehicle and ABX mice. The data are presented as the mean ± SEM of 7 mice, **p<0.01 compared with vehicle mice by Student's t-test.

However, antibiotic treatment did not affect the morphology of small intestine and colon as shown by the comparable length of small intestine and colon between vehicle and ABX mice. In addition, ABX model did not caused antibiotic-induced diarrhea.

Antibiotic treatment for 10 days caused a significant decrease approximately 20.8 ± 3.4% of GPR41-immunoreactivities in ABX mice compared with vehicle mice (Figure 24A and 24B; n=6-7; P<0.01).

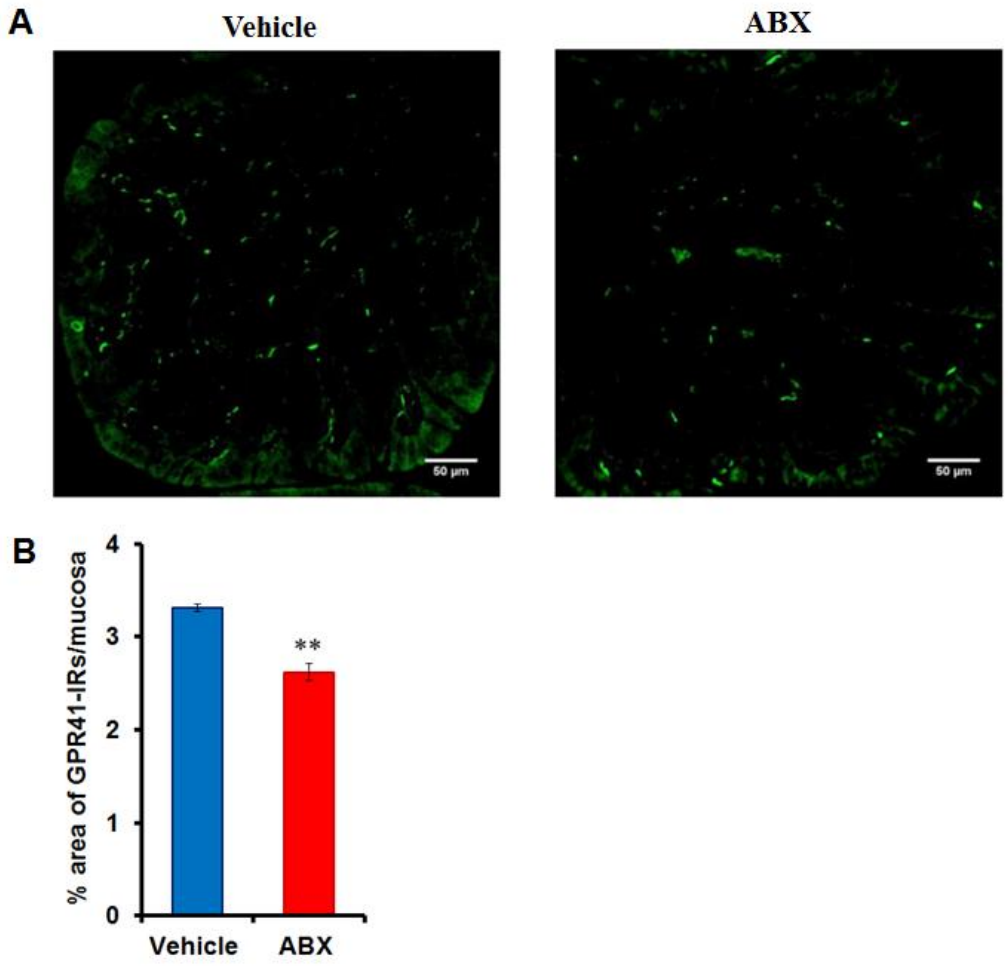

Figure 24. Antibiotic treatment for 10 days decreased the expression of GPR41 in ABX-treated mice. The data are presented as the mean ± SEM of 6-7 mice, **p<0.01 compared with vehicle mice by Student's t-test.

CGRP expression in the colonic lamina propria of ABX mice was significantly reduced by 24.2 ± 3.6% compared with vehicle-treated mice (Figure 25A and 25B; n=6-7; P<0.01).

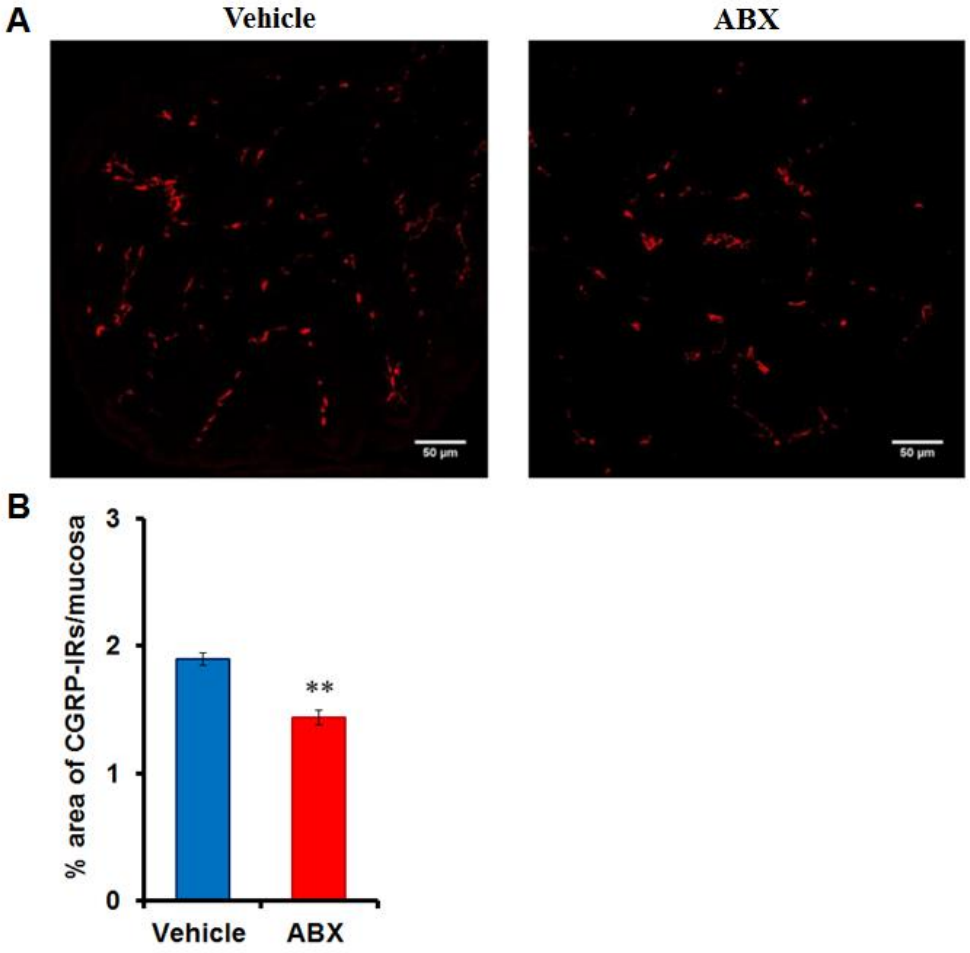

Figure 25. Antibiotic treatment for 10 days decreased the expression of CGRP in ABX-treated mice. Data are presented as the mean ± SEM of 6-7 mice, **p<0.01 compared with vehicle mice by Student's t-test.

I observed colocalization between GPR41-IRs and CGRP-IRs in the colonic lamina propria of vehicle and ABX mice (Figure 26A). The ratio of double-positive IRs to GPR41-IRs or CGRP-IRs was unaffected by antibiotic treatment (Figure 26B and 26C).

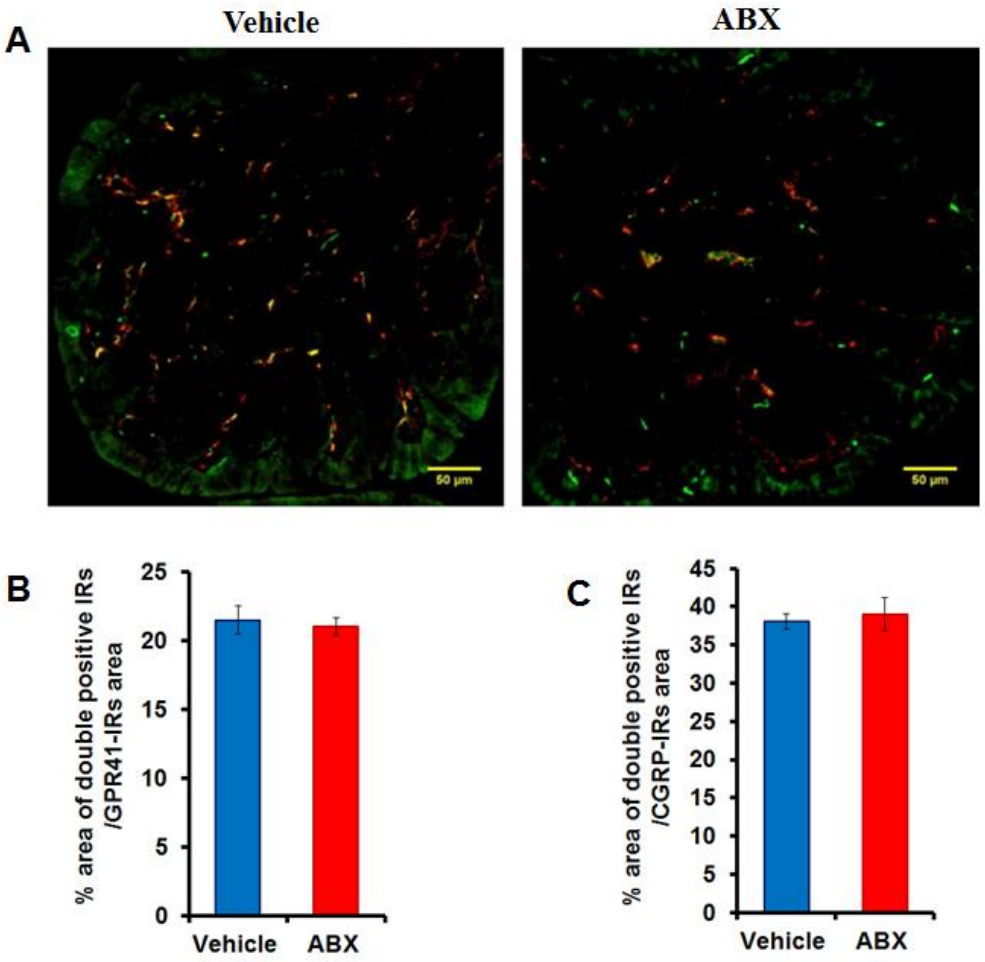

Figure 26. Colocalization between GPR41 and CGRP were found in the colonic lamina propria of a vehicle and ABX-treated mice. (A) Representative images of double-positive IRs of GPR41 and CGRP in the colonic lamina propria and muscularis layer of mice colon after antibiotic treatment for 10 days. (B) Quantitative analysis of double-positive IRs/GPR41 IRs area. (C) Quantitative analysis of double-positive IRs/CGRP IRs area. The data are presented as the mean ± SEM of 6-7 mice.

4. Discussion

DSS-induced colitis model is known as the most widespread and most characterized chemically induced models in the investigation of inflammation related to UC (Solomon et al., 2010; Chassaing et al., 2014). Most of the DSS model studies focused on mucosal response affected by DSS treatment and its similarity to clinical manifestation found in UC patients (Munyaka et al., 2016; Wirtz and Neurath, 2007; Kitajima et al., 2000; Melgar et al., 2008; Yan et al., 2009). Only several studies of the DSS model investigated the dysbiosis of the gut microbiota and changes in their metabolic capacity related to DSS treatment (Munyaka et al., 2016; Berry et al., 2012; Smith et al., 2012). Those previous research revealed that DSS-induced colitis was associated with changes in the composition of gut microbiota and that gut microbiota could affect the sensitivity of the host to DSS treatment.

Our recent study showed that the colitis mice experienced severe colitis which was shown from body weight, DAI score, and destruction of epithelial integrity which accompanied by crypt architecture damaged.

My current reports indicate that GPR41 is expressed in both nerve fibers and cell somas of enteric neurons. Our results have a discrepancy with the previous findings using GPR41-mRFP transgenic mice which mentioned that GPR41 is expressed in the cell somas of submucosal neurons and myenteric neurons (Nøhr et al., 2013). This discrepancy probably due to the great difference in the sensitivity and accuracy required to detect GPR41 in the nerve fibers of mice colonic mucosa.

Prior reports related to GPR41 expression did not provide information on which type of enteric neurons expressed GPR41. The enteric nervous system, comprised of many types of neurons, such as intrinsic sensory neurons, interneurons, and motor neurons (Qu et al., 2008). These neurons configured intrinsic neural circuits and play a crucial role in the maintenance of gut integrity which largely depends on the rapid alarm from sensory neurons in the gut (Holzer, 2007). My study uses an anti-CGRP antibody to investigate whether GPR41 is expressed in intrinsic sensory neurons rather than enteric cholinergic neurons in the colonic mucosa. CGRP is assumed to be a neurotransmitter in cholinergic intrinsic sensory neurons in the mouse enteric nervous system (Lee et al., 2013; Qu et al., 2008). It is well known that

the local release of CGRP from terminals of sensory neurons is critical for the development of neurogenic inflammation. Furthermore, our previous study indicates that CGRP functions in the intestine as a mediator between the nervous system and immune system in a murine food allergy (FA) model (Lee et al., 2013). In my current research, CGRP-IRs were observed in the nerve fibers of the colonic lamina propria and it was significantly increased in mice with colitis. These results are in close agreement with our previous report which revealed that CGRP-immunoreactive nerve fibers juxtaposed with mucosal mast cells are specifically increased in the colonic mucosa of FA mice (Lee et al., 2013).

DSS-induced colitis reportedly causes the overgrowth of commensal enterobacteria such as Escherichia coli which possesses potential proinflammatory properties (Heimesaat et al., 2011). Toll-like receptor-4, which recognizes lipopolysaccharide (membrane component of gram-negative bacteria) is reportedly expressed in myenteric neurons of the mouse colon (Barajon et al., 2009), suggesting that enteric neural circuits might be directly activated by enteric bacteria. One possible explanation for the increased GPR41 and CGRP expression after DSS treatment is due to activation of enteric neurons, especially sensory neurons, by easy penetration of SCFAs and enteric bacteria into the lamina propria through colitis-induced disruption of the epithelial barrier function in the colon of mice with colitis.

My recent research found the colocalization between GPR41 and CGRP in mice colonic lamina propria indicated that GPR41 is located in the nerve fibers and cell somas of cholinergic intrinsic sensory neurons in the mouse colon. The ratio of double-positive IRs to GPR41-IRs or CGRP-IRs is suggested that GPR41 expression in nerve fibers of enteric neurons other than sensory neurons is upregulated by DSS treatment, which may cause a disturbance of intrinsic neural circuits and subsequently result in disorders of colonic motility such as diarrhea that are typically observed in colitis mice.

The mechanisms and pathways that are probably related to GPR41 involvement in the pathology of enteric immune disorders remain elusive. In this recent research, I observed F4/80-positive intestinal macrophages were located in the colonic lamina propria of colitis mice. The proportion of these intestinal macrophages was markedly upregulated in the colonic mucosa after DSS treatment compared with normal mice. This result was in

agreement with our previous report (Hayashi et al., 2017). Many GPR41-immunoreactive nerve fibers found in the colonic lamina propria were juxtaposed with F4/80-positive macrophages. Our previous report in food allergy model mice indicated that CGRP-positive intrinsic sensory neurons were involved in the pathogenesis of food allergy via neuro-immune interaction with mucosal mast cells (Lee et al., 2013; Kim et al., 2014; Yamamoto et al., 2014). In addition, it is reported that microbiota-driven crosstalk between muscularis macrophages and enteric neurons regulates gastrointestinal motility (Muller et al., 2014). Taken together, these results indicated that neuro-immune interaction of GPR41-positive intrinsic sensory neurons and F4/80-positive macrophages in the colonic lamina propria might contribute to the maintenance of intestinal homeostasis and the pathogenesis of intestinal immune disorders accompanied by gut microbiota dysbiosis.

ABX model is frequently used to investigate the gut microbiota interaction with the host in terms of intestinal homeostasis, luminal signaling, and metabolism. ABX model is considered to be a more reasonable model to investigate the causative of gut microbiota-dependent effect compared with the germ-free mouse model. GPR41 downregulation in the colonic lamina propria of ABX-treated mice probably due to the reduced number of enteric bacteria and gut microbiota composition change after antibiotic treatment. A previous report showed gut microbiota composition in normal mice is dominated by Firmicutes species (butyrate-producing bacteria) and Bacteroidetes species, meanwhile, it is shifted to Proteobacteria after antibiotic treatment (Zarrinpar et al., 2018). CGRP expression in colonic lamina propria was also reduced in ABX mice compared to vehicle mice. GPR41-IRs was found to be colocalized with CGRP-IRs in the colonic lamina propria of the vehicle and ABX-treated mice. The ratio of double-positive IRs to GPR41-IRs or CGRP-IRs was unaffected by antibiotic treatment, indicated that antibiotic treatment for 10 days did not affect the composition of either GPR41-positive fibers or CGRP-positive sensory nerve fibers. In addition antibiotic treatment also did not generate antibiotic-induced diarrhea, suggesting that antibiotic-induced dysbiosis may not influence enteric neural circuits.

Taken together, I conclude that GPR41-positive nerve fibers might be act as a mediator in the crosstalk between host immune system and gut microbiota. Besides, neuro-immune

interaction were shown by the GPR41-positive nerve fibers juxtaposed with F4/80-positive macrophages (Figure 27).

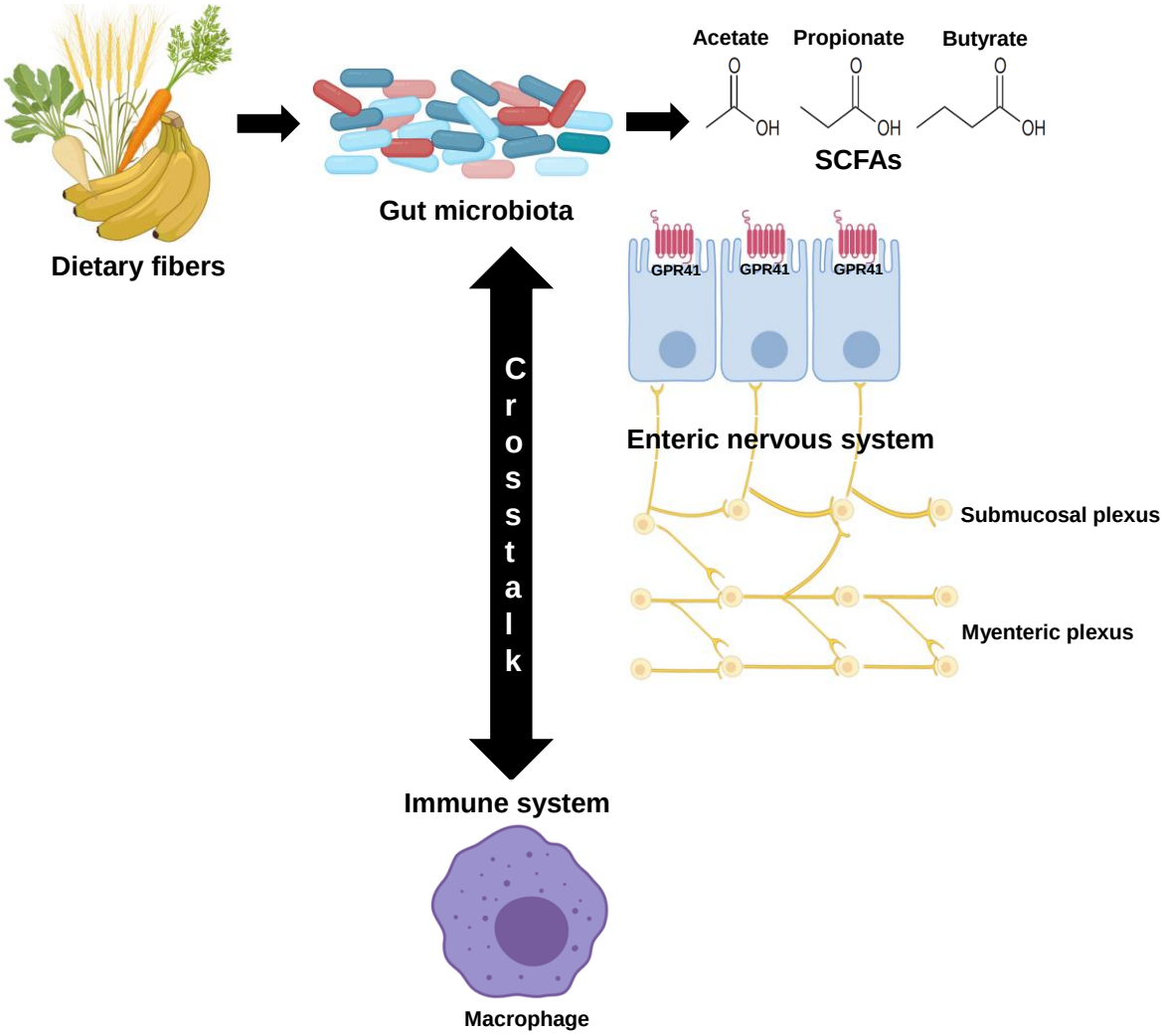

Figure 27. Schematic representation of how GPR41 acts as a mediator of crosstalk between gut microbiota and immune system in the gastrointestinal tract through activation by SCFAs which is generated from the fermentation of dietary fibers by gut microbiota.

Conclusion and Future Directions

My recent report to study the pathophysiological role of IL-4Rα and GPR41 in the murine colitis model reveals some important findings.

The first study to investigate the role of IL-4Rα seems to be the first time to show the role of interleukin 4 receptor alpha in the intestinal inflammation in vivo. An important finding from my study is depletion of IL-4R alpha elevated ROS production-derived NOX1 and modulate intestinal mucosal barrier function, resulting the alleviation of acute colitis severity (Figure 15). The limitation of this study is I could not show direct evidence that epithelial cells indeed produced ROS-derived NOX1 to protect the IL-4Rα-/- mice from colitis. Accumulating evidence from previous reports mentioned that IBD therapy aims is to create a long-term remission state, and to address this objective reconstruction of a wounded intestinal mucosa is required after induction of remission (Neurath and Travis, 2012). My findings could contribute to a novel therapeutic strategy by creating long-term remission through the regulation of ROS production-derived NOX1 mediated by IL-4α signaling (Figure 28).

My second study which aimed to determined pathophysiological roles of GPR41 in the intestinal inflammation demonstrated for the first time that GPR41 was expressed by enteric nerve fibers of both the lamina propria and muscularis layer of mice beside the cell soma of enteric neurons. My study also revealed that GPR41 is expressed on a part of cholinergic enteric sensory neurons which showed by the results in Figure 20 and 26 that approximately one-third of CGRP immunoreactive nerve fibers were immunoreactive for GPR41. GPR41-positive nerve fibers were found in close proximity with F4/80-positive nerve fibers indicated that neuro-immune interaction of GPR41-positive intrinsic sensory neurons and F4/80-positive macrophages probably contribute to the maintenance of intestinal homeostasis and the pathogenesis of intestinal inflammation accompanied by gut microbiota dysbiosis. My finding could contribute as preliminary data for further experiments to elucidate whether the GPR41 expression plays a functional role in the development of intestinal inflammation in the future.

In conclusion, although further research is needed to clarify the mechanism of intestinal mucosal barrier function regulation by IL-4Rα and GPR41, the results of this study are expected to get a deeper understanding of IBD pathogenesis. My current finding might play contribution to create a novel therapeutic approach for IBD treatment (Figure 28).

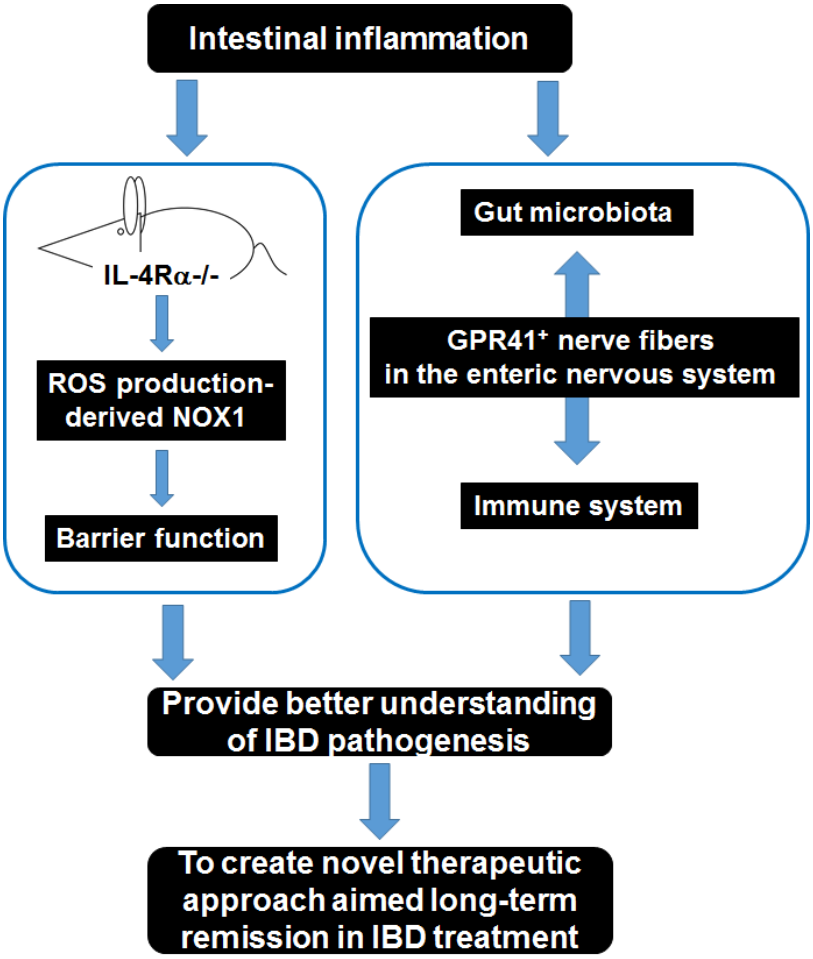

Figure 28. Depiction image how the finding in the role of IL-4Rα and morphological alteration of GPR41 in the intestinal inflammation may improve the understanding of IBD pathogenesis and contribute to create novel therapy in IBD treatment.

References

Baumgart, D. C and Carding, S. R. (2007). Inflammatory bowel disease: cause and immunobiology. *Lancet* 369, 1627-1640. doi: 10.1016/S0140-6736(07)60750-8

Lee, S. H., Kwon, J. E., & Cho, M. L. (2018). Immunological pathogenesis of inflammatory bowel disease. *Intest Res*, 16(1), 26–42. doi:10.5217/ir.2018.16.1.26

De Souza, H.S and Fiocchi, C. (2016). Immunopathogenesis of IBD: current state of the art. *Nat Rev Gastroenterol Hepatol* 13, 13-27. doi: 10.1038/nrgastro.2015.186

Levine, A., Griffiths, A., Markowitz, J., Wilson, D.C., Turner, D., Russel, R.K., et al. (2011). Pediatric modification of the Montreal classification for inflammatory bowel disease: the Paris classification. *Inflamm Bowel Dis* 17, 1314-1321. doi: 10.1002/ibd.21493

Ng, C. S., Shi, H. Y., Hamidi, N., Underwood, F. E., Tang, W., Benchimol, E. I., et al. (2017). Worldwide incidence and prevalence of inflammatory bowel disease in the 21st century: a systematic review of population-based studies. *The Lancet* 390, 2769-2778, doi: org/10.1016/S0140-6736(17)32448-0

Benchimol, E.I., Fortinsky, K.J., Godzyra, P., Heuvel, M.V., Limbergen, J.V., Griffiths, A.M. (2011). Epidemiology of pediatric inflammatory bowel disease: a systematic review of international trends. *Inflamm Bowel Dis* 17, 423-439. doi: 10.1002/ibd.21349

Benchimol, E.I., Mack, D.R., Nguyen, G.C., Snapper, S.B., Li, W., Mojaverian, N., et al. (2014). Incidence, outcomes, and health services burden of very early onset inflammatory bowel disease. *Gastroenterology* 147, 803-813. e807. doi: 10.1053/j.gastro.2014.06.023

Alatab, S., Sepanlou, S.G., Ikuta, K., Vahedi, H., Bisignano, C., Safiri, S., et al. (2020). The global, regional, and national burden of inflammatory bowel disease in 195 countries and territories, 1990–2017: a systematic analysis for the global burden of disease study 2017. *Lancet Gastroenterol Hepatol* 5, 17–30. doi: 10.1016/S2468-1253(19)30333-4

Okabayashi, S., Kobayashi, T., & Hibi, T. (2020). Inflammatory bowel disease in Japan-is it similar to or different from westerns? *JARC* 4, 1–13. doi:10.23922/jarc.2019-003

Kumar, M., Garand, M., Al Khodor, S. (2019). Integrating omics for a better understanding of inflammatory bowel disease: a step towards personalized medicine. *J Transl Med* 17, 419. doi: 10.1186/s12967-019-02174-1

Neurath, M. F., and Travis, S. P. (2012). Mucosal healing in inflammatory bowel diseases: a systematic review. *Gut* 61, 1619-1635. doi: 10.1136/gutjnl-2012-302830

Sartor, R.B. (2006). Mechanisms of disease: pathogenesis of Crohn's disease and ulcerative colitis. *Nat Clin Pract Gastroenterol Hepatol* 3, 390-407. doi: 10.1038/ncpgasthep0528

Schoultz, I., Keita, Å.V., (2020). The intestinal barrier and current techniques for the assessment of gut permeability. *Cells*. 9, 1909. doi: 10.3390/cells9081909

Furness, J.B., Kunze, W.A., Clerc, N. (1999). Nutrient tasting and signaling mechanisms in the gut. II. The intestine as a sensory organ: Neural, endocrine, and immune responses. *Am J Physiol* 277, G922–G928. doi: 10.1152/ajpgi.1999.277.5.G922

Cornick, S.; Tawiah, A.; Chadee, K. (2015). Roles and regulation of the mucus barrier in the gut. *Tissue Barriers* 3, e982426. doi: 10.4161/21688370.2014.982426

Smith, H.F., Fisher, R.E., Everett, M.L., Thomas, A.D., Bollinger, R.R., Parker, W. (2009). Comparative anatomy and phylogenetic distribution of the mammalian cecal appendix. *J Evol Biol* 22, 1984–1999. doi: 10.1111/j.1420-9101.2009.01809.x

Gutzeit, C.; Magri, G.; Cerutti, A. (2014). Intestinal IgA production and its role in host-microbe interaction. *Immunol Rev* 260, 76–85. doi: 10.1111/imr.12189

Schoultz, I.; Keita, Å.V. (2019). Cellular and molecular therapeutic targets in inflammatory bowel disease-focusing on intestinal barrier function. *Cells* 8, 193. doi: 10.3390/cells8020193

Santaolalla, R., Fukata, M., Abreu, M. T. (2011). Innate immunity in the small intestine. *Curr Opin Gastroenterol* 27, 125-131. doi: 10.1097/MOG.0b013e3283438dea

Okumura, R., and Takeda, K. (2017). Roles of intestinal epithelial cells in the maintenance of gut homeostasis. *Exp Mol Med* 49, e338. doi: 10.1038/emm.2017.20

Quiros, M., and Nusrat, A. (2019). Saving problematic Mucosae: SPMs in intestinal mucosal inflammation and repair. *Trend Mol Med* 25, 124-135. doi: 10.1016/j.molmed.2018.12.004

Friedrich, M., Pohin, M., and Powrie, F. (2019). Cytokine networks in the pathophysiology of inflammatory bowel disease. *Immunity* 50, 992-1006. doi: 10.1016/j.immuni.2019.03.017

D'Souza, W.N., Douangpanya, J., Mu, S., Jaeckel, P., Zhang, M., Maxwell, J. R., et al. (2017). Differing roles for short chain fatty acids and GPR43 agonism in the regulation of intestinal barrier function and immune responses. *PLoS One* 12, e0180190. doi:10.1371/journal.pone.0180190

Egholm, C., Heeb, L. E. M., Impellizzieri, D., and Boyman, O. (2019). The regulatory effects of interleukin-4 receptor signaling on neutrophils in type 2 immune responses. *Front Immunol* 10, 2507. doi: 10.3389/fimmu.2019.02507

LaPorte, S. L., Juo, Z. S., Vaclavikova, J., Colf, L. A., Qi, X., Heller, N. M., et al. (2008). Molecular and structural basis of cytokine receptor pleiotropy in the interleukin-4/13 system. *Cell* 132, 259-272. doi: 10.1016/j.cell.2007.12.030

Nelms, K., Keegan, A.D., Zamorano, J., Ryan, J.J., Paul, W.E. (1999). The IL-4 receptor: signaling mechanisms and biologic functions. *Annu Rev Immunol* 17, 701-738. doi: 10.1146/annurev.immunol.17.1.701

Takeda, K., Hashimoto, K., Uchikawa, R., Tegoshi, T., Yamada, M., and Arizono, N. (2010). Direct effects of IL-4/IL-13 and the nematode Nippostrongylus brasiliensis on intestinal epithelial cells in vitro. *Parasite Immunol* 32, 420-429. doi: 10.1111/j.1365-3024.2010.01200.x

Jenkins, S. J., Ruckerl, D., Thomas, G. D., Hewitson, J. P., Duncan, S., Brombacher, F., et al. (2013). IL-4 directly signals tissue-resident macrophages to proliferate beyond homeostatic levels controlled by CSF-1. *J Exp Med* 210, 2477-2491. doi: 10.1084/jem.20121999

Lee, H. K., Koh, S., Lo, D. C., and Marchuk, D. A. (2018). Neuronal IL-4Rα modulates neuronal apoptosis and cell viability during the acute phases of cerebral ischemia. *FEBS J* 285, 2785-2798. doi: 10.1111/febs.14498

Groschwitz, K. R., and Hogan, S. P. (2009). Intestinal barrier function: molecular regulation and disease pathogenesis. *J Allergy Clin Immunol* 124, 3-20. doi: 10.1016/j.jaci.2009.05.038

Heller, F., Florian, P., Bojarski, C., Richter, J., Christ, M., and Hillenbrand, B., et al. (2005). Interleukin-13 is the key effector Th2 cytokine in ulcerative colitis that affects epithelial tight junctions, apoptosis, and cell restitution. *Gastroenterology* 129, 550-564. doi: 10.1016/j.gastro.2005.05.002

Le Poul, E., Loison, C., Struyf, S., Springael, J.Y., Lannoy, V., Decobecq, M.E., et al. (2003). Functional characterization of human receptors for short chain fatty acids and their role in polymorphonuclear cell activation. *J Biol Chem* 278, 25481-9. doi: 10.1074/jbc.M301403200

Brown, A.J., Goldsworthy, S. M., Barnes, A.A., Eilert, M.M., Tcheang, L., Daniels, D., et al. (2003). The orphan G protein-coupled receptors GPR41 and GPR43 are activated by propionate and other short chain carboxylic acids, *J Biol Chem* 278, 11312-9. doi: 10.1074/jbc.M211609200

Kimura, I., Inoue, D., Maeda, T., Hara, T., Ichimura, A., Miyauchi, S., et al. (2011). Short-chain fatty acids and ketones directly regulate sympathetic nervous system via G protein-coupled receptor 41 (GPR41). *Proc Natl Acad Sci USA* 108, 8030–8035. doi:10.1073/pnas.1016088108

Samuel, B.S., Shaito, A., Motoike, T., Rey, F.E., Backhed,F., Manchester, J.K., et al. (2008). Effects of the gut microbiota on host adiposity are modulated by the short-chain fatty-acid

binding G protein-coupled receptor, Gpr41. *Proc Natl Acad Sci USA* 105, 16767–16772. doi:10.1073/pnas.0808567105

Scheppach, W. (1994). Effects of short chain fatty acids on gut morphology and function. *Gut*. 35 (1 Suppl), S35-8. doi: 10.1136/gut.35.1_suppl.s35

Priyadarshini, M., Kotlo, K.U., Dudeja, P.K., Layden, B.T. (2018). Role of Short Chain Fatty Acid Receptors in Intestinal Physiology and Pathophysiology. *Compr Physiol* 8, 091-1115. doi:10.1002/cphy.c170050

Nilsson, N.E., Kotarsky, K., Owman, C., Olde, B. (2003). Identification of a free fatty acid receptor, FFA2R, expressed on leucocytes and activates by short-chain fatty acids. *Biochem Biophys Res Commun* 4, 1047-52. doi: 10.1016/s0006-291x(03)00488-1

Thangaraju, M., Cresci, G.A., Liu, K., Ananth, S., Gnanaprakasam, J.P., Browning, D.D., et al. (2009). GPR109A is a G-protein-coupled receptor for the bacterial fermentation product butyrate and functions as a tumor suppressor in the colon. *Cancer Res* 69, 2826-32. doi: 101158/0008-5472.CAN-08-4466

Arpaia, N., Campbell, C., Fan, X., Dikiy, D., van der Veeken, J., deRoos, P., et al. (2013). Metabolites produced by commensal bacteria promote peripheral regulatory T-cell generation. *Nature* 504, 451-5. doi: 10.1038/nature12726

Maslowski, K. M., Vieira, A. T., Ng, A., Kranich, J., Sierro, F., Yu, D., et al. (2009). Regulation of inflammatory responses by gut microbiota and chemoattractant receptor GPR43. *Nature* 461 (7268), 1282-6. doi: 10.1038/nature08530

Masui, R., Sasaki, M., Funaki, Y., Ogasawara, N., Mizuno, M., Iida, A., et al. (2013). G protein-coupled receptor 43 moderates gut inflammation through cytokine regulation from mononuclear cells. *Inflamm Bowel Dis* 19, 2848-56. doi: 10.1097/01.MIB.000435444.14860.ea

Okayasu I, Hatakeyama S, Yamada M, Ohkusa T, Inagaki Y, Nakaya R. (1990). A novel method in the induction of reliable experimental acute and chronic ulcerative colitis in mice. *Gastroenterology* 98, 694–702

Chassaing, B., Aitken, J. D., Malleshappa, M., & Vijay-Kumar, M. (2014). Dextran sulfate sodium (DSS)-induced colitis in mice. *Curr Protoc Immunol* 104, 15.25.1–15.25.14. doi: 10.1002/0471142735.im1525s104

Yan,Y., Kolachala, V., Dalmasso, G., Ngyuyen, H., Laroui, H., Sitaraman, S.V., Merlin, D. (2009). Temporal and spatial analysis of clinical and molecular parameters in dextran sodium sulfate induced colitis," *PLoS One* 4, e6073. doi: 10.1371/journal.pone.0006073

Perše, M., Cerar, A. (2012). Dextran sodium sulphate colitis mouse model: traps and tricks. *BioMed Res Int* 2012, doi: 10.1155/2012/718617

Melgar, S., Karlsson, A., and Michaëlsson, E. (2005). Acute colitis induced by dextran sulfate sodium progresses to chronicity in C57BL/6 but not in BALB/c mice: correlation between symptoms and inflammation. *Am J Physiol Gastrointest Liver Physiol* 288, G1328-G1338. doi: 10.1152/ajpgi.00467.2004

Hayashi, S., Hamada, T., Zinsou, D. G. A., Oshiro, M., Itoi, K., Yamamoto, T., et al. (2017). PI3K p85α subunit-deficient macrophages protect mice from acute colitis due to the enhancement of IL-10 production. *Sci Rep* 7, 6187. doi: 10.1038/s41598-017-06464-w

Farooq, S.M., Stillie, R., Svensson, M., Svanborg, C., Strieter, R. M., and Stadnyk, A. W. (2009). Therapeutic effect of blocking CXCR2 on neutrophil recruitment and dextran sodium sulfate-induced colitis. *J Pharmacol Exp Ther* 329, 123-129. doi: 10.1124/jpet.108.145862

Zarrinpar, A., Chaix, A., Xu, Z.Z., Chang, M. W., Marotz, C.A., Saghatelian, A., Knight, R., Panda, S. (2018). Antibiotic-induced microbiome depletion alters metabolic homeostasis by affecting gut signaling and colonic metabolism. *Nat Commun* 9, 2872. doi: 10.1038/s41598-017-06464-w

Sampson, T.R., Debelius, J. W., Thron, T., Jansen, S., Shastri, G.G., Ilhan, Z.E., et al. (2016). Gut microbiota regulate motor deficits and neuroinflammation in a model of Parkinson's disease. *Cell* 167, 1469–1480e1412. doi: 10.1016/j.cell.2016.11.018

Shen, T. C., Albenberg, L., Bittinger, K., Chehoud, C., Chen, Y. Y., Judge, C. A., Chau, L., Ni, J., Sheng, M., Lin, A., Wilkins, B. J., Buza, E. L., Lewis, J. D., Daikhin, Y., Nissim, I., Yudkoff, M., Bushman, F. D., & Wu, G. D. (2015). Engineering the gut microbiota to treat hyperammonemia. *J Clin Invest* 125, 2841–2850. doi: 10.1172/JCI79214

Rakoff-Nahoum, S., Paglino, J., Eslami-Varzaneh, F., Edberg, S., Medzhitov, R. (2004). Recognition of commensal microflora by toll-like receptors is required for intestinal homeostasis. *Cell* 118, 229–241. doi: 10.1016/j.cell.2004.07.002

Mahana, D., Trent, C.M., Kurtz, Z.D., Bokulich, N.A., Battaglia, T., Chung, J., et al. (2016). Antibiotic perturbation of the murine gut microbiome enhances the adiposity, insulin resistance, and liver disease associated with high-fat diet. *Genome Med* 8, 48. doi: 10.1186/s13073-016-0297-9

Cho, I., Yamanishi, S., Cox, L., Methé, B.A., Zavadil, J., Li, K., et al. (2012). Antibiotics in early life alter the murine colonic microbiome and adiposity. *Nature* 488, 621–626. doi: 10.1038/nature11400

Cox, L. M., Yamanishi, S., Sohn, J., Alekseyenko, A.V., Leung, J.M., Cho, I., et al. (2014). Altering the intestinal microbiota during a critical developmental window has lasting metabolic consequences. *Cell* 158, 705–721. doi: 10.1016/j.cell.2014.05.052

Holota Y, Dovbynchuk T, Kaji I, Vareniuk, I, Dzyubenko N, Chervinska T, et al. (2019) The long-term consequences of antibiotic therapy: role of colonic short-chain fatty acids (SCFA) system and intestinal barrier integrity. *PLoS One* 14(8): e0220642. doi: 10.1371/journal. pone.0220642

Canfora, E. E., Jocken, J. W. & Blaak E. E. (2015). Short-chain fatty acids in control of body weight and insulin sensitivity. *Nat Rev Endocrinol* 10, 577-591. doi: 10.1038/nrendo.2015.128

Wichmann, A., Allahyar, A., Greiner, T. U., Plovier, H., Lundén, G. Ö., Larsson, et al. (2013). Microbial modulation of energy availability in the colon regulates intestinal transit. *Cell host & microbe*, *14*(5), 582–590. doi: 10.1016/j.chom.2013.09.012

Bäckhed, F., Manchester, J. K., Semenkovich, C. F., Gordon, J. I. (2007). Mechanisms underlying the resistance to diet-induced obesity in germ-free mice. *Proc Natl Acad Sci USA* 104, 979–984. doi: 10.1073/pnas.0605374104

Zünd, G., Madara, J. L., Dzus, A. L., Awtrey, C. S., and Colgan, S. P. (1996). Interleuin-4 and interleukin-13 differentially regulate epithelial chloride secretion. *J Biol Chem* 271, 7460-7464. doi: 10.1074/jbc.271.13.7460

Berin, M. C., Yang, P. C., Ciok, L., Waserman, S., Perdue, M. H. (1999). Role for IL-4 in macromolecular transport across human intestinal epithelium. *Am J Physiol* 276, C1046-1052, 1999. doi: 10.1152/ajpcell.1999.276.5.C1046

Madden, K. B., Whitman, L., Sullivan, C., Gause, W. C., Urban, J. F., Katona, I. M. (2002). Role of STAT6 and mast cells in IL-4- and IL-13-induced alterations in murine intestinal epithelial cell function. *J Immunol* 169, 4417-4422. doi: 10.4049/jimmunol.169.8.4417

Cummings, J.H., Antoine, J.M., Azpiroz, F., Bourdet-Sicard, R., Brandtzaeg, P., Calder, P.C., et al. (2004). PASSCLAIM–gut health and immunity. *Eur J Nutr* 43, II118–II173. doi: 10.1007/s00394-004-1205-4

Bischoff, S.C., Barbara, G., Buurman, W., Ockhuizen, T., Schulzke, J-D., Serino, M., et al. (2014). Intestinal permeability- a new target for disease prevention and therapy. *BMC Gastroenterol* 14, 189. doi: 10.1186/s12876-014-0189-7

Hooper, L.V., Macpherson, A.J. (2010). Immune adaptations that maintain homeostasis with the intestinal microbiota. *Nature Rev Immunol* 10, 159-169. doi: 10.1038/nri2710

Koslowski, M.J., Beisner, J., Stange, E.F., Wehkamp, J. (2010). Innate microbial host defense in small intestinal Crohn's disease. *Int J Med Microbiol* 300, 34-40. doi: 10.1016/j.ijmm.2009.08.011

Martini, E., Krug, S.M., Siegmund, B., Neurath, M.F., Becker, C. (2017). Mend your fences: the epithelial barrier and its relationship with mucosal immunity in inflammatory bowel disease. *Cell Mol Gastroenterol Hepatol* 4, 33-46. doi: 10.1016/j.jcmgh.2017.03.007

Noben-Trauth, N., Shultz, L. D., Brombacher, F., Urban, J. F. Jr, Gu, H., Paul, W. E. (1997). An interleukin 4 (IL-4)-independent pathway for CD4+ T cell IL-4 production is revealed in IL-4 receptor-deficient mice. *Proc Natl Acad Sci USA* 94, 10838-10843. doi: 10.1073/pnas.94.20.10838

Hayashi, S., Hamada, T., Zaidi, S. F., Oshiro, M., Lee, J., Yamamoto, T., et al. (2014). Nicotine suppresses acute colitis and colonic tumorigenesis associated with chronic colitis in mice. *Am J Physiol Gastrointest Liver Physiol* 307, G968-G978. doi: 10.1152/ajpgi.00346.2013

Lee, J., Yamamoto, T., Hayashi, S., Kuramoto, H., and Kadowaki, M. (2013). Enhancement of CGRP sensory afferent innervation in the gut during the development of food allergy in an experimental murine model. *Biochem Biophys Res Commun* 430, 895-900. doi: 10.1016/j.bbrc.2012.12.058

Nagata, Y., Yamamoto, T., Hayashi, M., Hayashi, S., and Kadowaki, M. (2017). Improvement of therapeutic efficacy of oral immunotherapy in combination with regulatory T cell-inducer kakkonto in a murine food allergy model. *PLoS One* 12, e0170577. doi: 10.1371/journal.pone.0170577

Greten, F. R., Eckmann, L., Greten, T. F., Park, J. M., Li, Z. W., Egan, L. J., et al.(2004). IKKbeta links inflammation and tumorigenesis in a mouse model of colitis-associated cancer. *Cell* 118, 285-296. doi: 10.1016/j.cell.2004.07.013

Yokota, H., Tsuzuki, A., Shimada, Y., Imai, A., Utsumi, D., Tsukahara, T., et al. (2017). NOX1/NADPH oxidase expressed in colonic macrophages contributes to the pathogenesis of colonic inflammation in trinitrobenzen sulfonic acid-induced murine colitis. *J Pharmacol Exp Ther* 360, 192-200. doi: 10.1124/jpet.116.235580

Gupta, J., del Barco Barrantes, I., Igea, A., Sakellariou, S., Pateras, I. S., Gorgoulis, V. G., et al. (2014). Dual function of p38α MAPK in colon cancer: suppression of colitis-associated tumor initiation but requirement for cancer cell survival. *Cancer Cell* 25, 484-500. doi: 10.1016/j.ccr.2014.02.019

Lambeth, J. D., and Neish, A. S. (2014). Nox enzymes and new thinking on reactive oxygen: a double-edged sword revisited. *Annu Rev Pathol* 9, 119-145. doi: 10.1146/annurev-pathol-012513-104651

Szanto, I., Rubbia-Brandt, L., Kiss, P., Steger, K., Banfi, B., Kovari, E., et al. (2005). Expression of NOX1, a superoxide-generating NADPH oxidase, in colon cancer and inflammatory bowel disease. *J Pathol* 207, 164-176. doi: 10.1002/path.1824

Valente, A. J., Zhou, Q., Lu, Z., He, W., Qiang, M., and Ma, W., et al. (2008). Regulation of NOX1 expression by GATA, HNF-1alpha, and Cdx transcription factors. *Free Radic Biol Med* 44, 430-443. doi: 10.1016/j.freeradbiomed.2007.10.035

Herbert, D.B.R., Hölscher, C., Mohrs, M., Arendse, B., Schwegmann, A., Radwanska, M., et al. (2004). Alternative macrophage activation is essential for survival during Schistosomiasis and downmodulates Thelper1 responses and immunopathology, *Immunity* 20, 623-635, doi: 10.1016/S1074-7613(04)00107-4

Maloy, K. J., and Powrie, F. (2011). Intestinal homeostasis and its breakdown in inflammatory bowel disease. *Nature* 474, 298-306. doi: 10.1038/nature10208

Kaser, A., Zeissig, S., and Blumberg, R. S. Inflammatory bowel disease. (2010). *Annu Rev Immunol* 28, 573-621. doi: 10.1146/annurev-immunol-030409-101225

Liu, J. Z., van Sommeren, S., Huang, H., Ng, S. C., Alberts, R., Takahashi, A., et al. (2015). International multiple sclerosis genetics consortium; international IBD genetics consortium: association analyses identify 38 susceptibility loci for inflammatory bowel disease and highlight shared genetic risk across populations. *Nat Genet* 47, 172-179. doi: 10.1038/ng.3176

Mizoguchi, A., Mizoguchi, E., and Bhan, A. K. (1999). The critical role of interleukin 4 but not interferon gamma in the pathogenesis of colitis in T-cell receptor alpha mutant mice. *Gastroenterology* 116, 320-326. doi: 10.1016/s0016-5085(99)70128-9

Heller, F., Fuss, I. J., Nieuwenhuis, E. E., Blumberg, R. S., and Strober, W. (2002). Oxazolone colitis, a Th2 colitis model resembling ulcerative colitis, is mediated by IL-13-producing NK-T cells. *Immunity* 17, 629-638. doi: 10.1016/s1074-7613(02)00453-3

Koller, F. L., Hwang, D. G., Dozier, E. A., Fingleton, B. (2010). Epithelial interleukin-4 receptor expression promotes colon tumor growth. *Carcinogenesis* 31, 1010-1017. doi: 10.1093/carcin/bgq044

Ohtsuka, Y., and Sanderson, I. R. (2003). Dextran sulfate sodium-induced inflammation is enhanced by intestinal epithelial cell chemokine expression in mice. *Pediatr Res* 53, 143-147. doi: 10.1203/00006450-200301000-00024

Wang, Y., Wang, K., Han, G. C., Wang, R. X., Xiao, H., Hou, C. M. et al. (2014). Neutrophil infiltration favors colitis-associated tumorigenesis by activating the interleukin-1 (IL-1)/IL-6 axis. *Mucosal Immunol* 7, 1106-1115. doi: 10.1038/mi.2013.126

Stevceva, L., Pavli, P., Husband, A., Ramsay, A., and Doe WF. (2001). Dextran sulphate sodium-induced colitis is ameliorated in interleukin 4 deficient mice. *Genes Immun* 2, 309-316. doi: 10.1038/sj.gene.6363782

Kim, H. S., and Chung, D. H. (2013). IL-9-producing invariant NKT cells protect against DSS-induced colitis in an IL-4-dependent manner. *Mucosal Immunol* 6, 347-357. doi: 10.1038/mi.2012.77

Hayes, P., Dhillon, S., O'Neill, K., Thoeni, C., Hui, K. Y., Elkadri, A., et al. (2015). Defects in NADPH oxidase genes NOX1 and DUOX2 in very early onset inflammatory bowel disease. *Cell Mol Gastroenterol Hepatol* 1, 489-502. doi: 10.1016/j.jcmgh.2015.06.005

Stenke, E., Bourke, B., and Knaus, U. G. (2019). NAPDH oxidases in inflammatory bowel disease. *Methods Mol Biol* 1982, 695-713. doi: 10.1007/978-1-4939-9424-3_38

Kühn, R., Löhler, J., Rennick, D., Rajewsky, K., and Müller, W. (1993). Interleukin-10-deficient mice develop chronic enterocolitis. *Cell* 75(2):263-274 doi: 10.1016/0092-8674(93)80068-p

Hayashi, S. (2020). Unraveling the pathogenesis of inflammatory bowel disease and search for new therapeutic medicines. *Yakugaku Zasshi* 140, 123-128. doi: 10.1248/yakushi.19-00164

Tréton, X., Pedruzzi, E., Guichard, C., Ladeiro, Y., Sedghi, S., Vallée, M., et al. (2014). Combined NADPH oxidase 1 and interleukin 10 deficiency induces chronic endoplasmic reticulum stress and causes ulcerative colitis-like disease in mice. *PLoS One* 9, e101669. doi: 10.1371/journal.pone.0101669

Aviello, G., Singh, A. K., O'Neill, S., Conroy, E., Gallagher, W., D'Agostino, G., et al. (2019). Colitis susceptibility in mice with reactive oxygen species deficiency is mediated by mucus barrier and immune defense defects. *Mucosal Immunol* 12, 1316-1326. doi: 10.1038/s41385-019-0205-x

Mouzaoui, S., Djerdjouri, B., Makhezer, N., Kroviarski, Y., El-Benna, J., and Dang, P. M. (2014). Tumor necrosis factor-α-induced colitis increases NADPH oxidase 1 expression, oxidative stress, and neutrophil recruitment in the colon: preventive effect of apocynin. *Mediators Inflamm* 2014, 312484. doi: 10.1155/2014/312484

Ramonaite, R., Skieceviciene, J., Juzenas, S., Salteniene, V., Kupcinskas, J., Matusevicius, P., et al. (2014). Protective action of NADPH oxidase inhibitors and role of NADPH oxidase

in pathogenesis of colon inflammation in mice. *World J Gastroenterol* 20, 12533-12541. doi: 10.3748/wjg.v20.i35.12533

Makhezer, N., Ben Khemis, M., Liu, D., Khichane, Y., Marzaioli, V., Tlili, A., et al. (2019). NOX1-derived ROS drive the expression of Lipocalin-2 in colonic epithelial cells in inflammatory conditions. *Mucosal Immunol* 12, 117-131. doi: 10.1038/s41385-018-0086-4

Levy, A., Stedman, A., Deutsch, E., Donnadieu, F., Virgin, H.W., Sansonetti, P.J., Nigro, G. (2020). Innate immune receptor NOD2 mediates LGR5+ intestinal stem cell protection against ROS cytotoxicity via mitophagy stimulation. *PNAS* 117, 1994-2003. doi: 10.1073/pnas.1902788117

Moll, F., Walter, M., Rezende, F., Helfinger, V., Vasconez, E., Oliveira, T.D., et al. (2018). NoxO1 controls proliferation of colon epithelial cells. *Front Immunol* 9, 973. doi:10.3389/fimmu.2018.00973

Cheung, E.C., Lee, P., Ceteci, F., Nixon, C., Blyth, K., Sansom, O.J., Vousden, K.H. (2015). Opposing effects of TIGAR- and RAC1-derived ROS on Wnt-driven proliferation in the mouse intestine. *Genes Dev* 30, 1-12

Leoni, G., Alam, A., Neumann, P. A., Lambeth, J. D., Cheng, G., McCoy, J., et al. (2013). Annexin A1, formyl peptide receptor, and NOX1 orchestrate epithelial repair. *J Clin Invest* 123, 443-454. doi: 10.1172/JCI65831

Coant, N., Ben Mkaddem, S., Pedruzzi, E., Guichard, C., Tréton, X., Ducroc, R., et al. (2010). NADPH oxidase 1 modulates WNT and NOTCH1 signaling to control the fate of proliferative progenitor cells in the colon. *Mol Cell Biol* 30, 2636-2650. doi: 10.1128/MCB.01194-09

Khoshnevisan, R., Anderson, M., Babcock, S., Anderson, S., Illig, D., Marquardt, B., et al. (2020). NOX1 regulates collective and planktonic cell migration: insights from patients with pediatric-onset IBD and NOX1 deficiency. *Inflamm Bowel Dis* 26, 1166-1176. doi: 10.1093/ibd/izaa017

Luissint, A. C., Parkos, C. A., and Nusrat, A. (2016). Inflammation and the intestinal barrier: leukocyte-epithelial cell interactions, cell junction remodeling, and mucosal repair. *Gastroenterology* 151, 616-632. doi: 10.1053/j.gastro.2016.07.008

Wilms, E., Troost, F.J., Elizalde, M., Winkens, B., de Vos, P., Mujagic, Z., Jonkers, D.M.A.E., Masclee, A.A.M. (2020). Intestinal barrier function is maintained with aging - a comprehensive study in healthy subjects and irritable bowel syndrome patients. *Sci Rep* 16, 475. doi: 10.1038/s41598-019-57106-2

Sharma, P., Charaborty, R., Wang, L., Min, B., Tremblay, M.L., Kawahara, T., et al. (2008). Redox regulation of interleukin 4 signaling. *Immunity* 29, 551-564. doi: 10.1016/j.immuni.2008.07.019

Liu, H., Antony, S., Roy, K, Juhasz, A., Wu, Y., Lu, J., et al. (2017). Interleukin-4 and interleukin-13 increase NADPH oxidase-1 related proliferation of human colon cancer cells. *Oncotarget* 8, 38113-38135

Machiels, K., Joossens, M., Sabino, J., Preter, V.D., Arijs, I., Eeckhaut, et al. (2014). A decrease of the butyrate-producing species Roseburia hominis and Faecalibacterium prausnitzii defines dysbiosis in patients with ulcerative colitis, *Gut* 63, 1275-1283. doi: 10.1136/gutjnl-2013-304833

Nishida, A., Inoue, R., Inatomi, O., Bamba, S., Naito, Y., Andoh, A. (2018). Gut microbiota in the pathogenesis of inflammatory bowel disease, *Clin J Gastroenterol* 11, 1-10. doi: 10.1007/s12328-017-0813-5

Kimura, I., Ichimura, A., Ohue-Itano, R., Igarashi, M. (2020). Free fatty acid receptors in health and disease. *Physiol Rev* 100, 171-210. doi: 10.1152/physrev.00041.2018

Ang, Z and Ding, J. K. (2016). GPR41 and GPR43 in obesity and inflammation – protective or causative? *Front Immunol* 7, 1-5. doi: 10.3389/fimmu.2016.00028

Nøhr, M. K., Pedersen, M. H., Gille, A., Egerod, K. L., Engelstoft, M. S., Husted, A. S., et al. (2013). GPR41/FFAR3 and GPR43/FFAR2 as cosensors for short-chain fatty acids in enteroendocrine cells vs FFAR3 in enteric neurons and FFAR2 in enteric leucocytes. *Endocrinology* 154, 3552-3564. doi: 10.1210/en.2013-1142

Munyaka, P.M., Rabbi, M.F., Khafipour, E., Ghia, J-E. (2016). Acute dextran sulfate sodium (DSS)-induced colitis promotes gut microbial dysbiosis in mice. *J Basic Microbiol* 56, 986-998. doi: 10.1002/jobm.201500726

Platt, A.N., Bain, C.C., Bordon, Y., Sester, D.P., Mowat, A.M. (2010). An independent subset of TLR expressing CCR2-dependent macrophages promotes colonic inflammation. *J Immunol* 184, 6843-6854. doi: 10.4049/jimmunol.0903987

Hill, D.A., Hoffmann, C., Abt, M.C., Du, Y., Kobuley, D., Kirn, T.J., Bushman, F.D., Artis, D. (2010). Metagenomic analyses reveal antibiotic-induced temporal and spatial changes in intestinal microbiota with associated alterations in immune cell homeostasis. *Mucosal Immunol* 3, 148-158. doi: 10.1038/mi.2009.132

Solomon, L., Mansor, S., Mallon, P., Donnelly, E., et al., (2010). The dextran sulphate sodium (DSS) model of colitis: an overview. *Comp Clin Pathol*, 19. 235-239. doi: 10.3748/wjg.v23.i33.6016

Wirtz, S., Neurath, M.F. (2007). Mouse models of inflammatory bowel disease. *Adv Drug Delivery Rev* 59, 1073-1083. doi: 10.1016/j.addr.2007.07.003

Kitajima, S., Takuma, S., Morimoto, M. (2000). Histological analysis of murine colitis induced by dextran sulfate sodium of different molecular weights. *Exp Anim* 49, 9-15. doi: 10.1538/expanim.49.9

Berry, D., Schwab, C., Milinovich, G., Reichert, J., et al. (2012). Phylotype-level 16S rRNA analysis reveal new bacterial indicators of health state in acute murine colitis. *ISME J* 6, 2091-2106. doi: 10.1038/ismej.2012.39

Smith, P., Siddarth, J., Pearson, R., Holway, N., et al. (2012). Host genetics and environmental factors regulate ecological succession of the mouse colon tissue-associated microbiota. *PLoS One* 7, e30273. doi: 10.1371/journal.pone.0030273

Qu, Z.D., Thacker, M., Castelucci, P., Bagyánszki, M., Epstein, M.L., Furness, J.B. (2008). Immunohistochemical analysis of neuron types in mouse small intestines, *Cell Tissue Res* 334, 147. doi: 10.1007/s00441-008-0684-7

Holzer, P. (2007). Role of visceral afferent neurons in mucosal inflammation and defence. *Curr Opin Pharmacol* 7, 563-569. doi: 10.1016/j.coph.2007.09.004

Yamamoto, T., Kodama, T., Lee, J., Utsunomiya, N., Hayashi, S., Sakamoto, H., Kuramoto, H., Kadowaki,M. (2014). Anti-allergic role of cholinergic neuronal pathway via α7 nicotinic ACh receptors on mucosal mast cells in a murine food allergy model. *PLoS One* 9, e85888. doi:10.1371/journal.pone.0085888

Kim, J.H., Yamamoto, T., Lee, J., Yashiro, T., Hamada, T., Hayashi, S., et al. (2014). CGRP, a neurotransmitter of enteric sensory neurons contributes to the development of food allergy due to the augmentation of microtubule reorganization in mucosal mast cells, *Biomed Res* 35, 285-93. doi:10.2220/biomedres.35.285

Muller, P.A., Koscso,B., Rajani, G.M., Stevanovic, K., Berres, M-L., Hashimoto, D., et al. (2014). Crosstalk between muscularis macrophages and enteric neurons regulates gastrointestinal motility. *Cell* 158, 300–313. doi: 10.1016/j.cell.2014.04.050

5. ACKNOWLEDGEMENTS

Firstly, I would like to express my sincere gratitude to my advisor Prof. Makoto Kadowaki for the continuous support of my Ph.D. study, for his patience, motivation, and immense knowledge. His guidance helped me in all the time of research and writing of this thesis.

Besides my advisor, I would like to thank my thesis committee: Prof. Toshiyasu Sasaoka, Prof. Yoshihiro Hayakawa, and Prof. Hiroaki Sakurai, for their insightful comments and encouragement, but also for the hard question which incented me to widen my research from various perspectives.

My deep and sincere gratitude to my supervisor Dr. Shusaku Hayashi who taught me how to perform and consider experiments as a researcher and for his great support and guidance in this work.

My sincere thanks also go to Dr. Takeshi Yamamoto for his valuable support and guidance in the laboratory.

I wish to thank my colleague Yudai Ogawa for his contribution and assistance in experiments. I am very thankful to all the research members of the "Division of Gastrointestinal Pathophysiology, Institute of Natural Medicine, Graduate School of Medicine and Pharmaceutical Sciences, University of Toyama" for sharing their skills, knowledge, and kindness with me. Without their precious support, it would not be possible to conduct this research. Thank you very much to the former member of the laboratory, Dr. Yuka Nagata for her friendship and support. I also really grateful to the staffs of University of Toyama who always give me support during my Ph.D. study.

Thank you very much for the RISET Pro, Ministry of Research and Technology of the Republic of Indonesia for providing scholarship during my Ph.D. study.

Last but not least I would like to thank my beloved husband for all the unconditional support, my mother for her love, my beloved sons, and my big brother. Thank you for always encouraging and support me to continue this study. My deep gratitude also for my brother Dede Erawan for inspiring me to study abroad since my childhood. Thank you very much for my sister in Indonesia, who always listens to me and gives me her precious support.